The sensitivity of Southern Ocean atmospheric dimethyl sulfide to modelled sources and emissions

Yusuf A. Bhatti[1], Laura E. Revell[1], Alex J. Schuddeboom[1,*], Adrian J. McDonald[1,2], Alex T. Archibald[3,4], Jonny Williams[5], Abhijith U. Venugopal[1], Catherine Hardacre[6,#], and Erik Behrens[5]

[1]School of Physical and Chemical Sciences, University of Canterbury, Christchurch, New Zealand
[2]Gateway Antarctica, University of Canterbury, Christchurch, New Zealand
[3]National Centre for Atmospheric Science, Cambridge, United Kingdom
[4]Yusuf Hamied Department of Chemistry, University of Cambridge, Cambridge, United Kingdom
[5]National Institute of Water and Atmospheric Research (NIWA), Wellington, New Zealand
[6]Met Office, Exeter, EX1 3PB, United Kingdom
[*]Now at National Institute of Water and Atmospheric Research (NIWA), Christchurch, New Zealand
[#]Now at School of Physical and Chemical Sciences, University of Canterbury, Christchurch, New Zealand

Correspondence: Yusuf Bhatti (yusuf.bhatti@pg.canterbury.ac.nz)

Abstract. The biogeochemical ~~behaviour~~ behavior of the Southern Ocean is complex and dynamic ~~. The processes that affect this behaviour are highly dependent on~~ and driven by physical, chemical, and biological ~~constraints, which are poorly constrained in Earth System Models. We assess how emissions~~ processes. Such processes leads to the formation of dimethyl sulfide (DMS), ~~a precursor~~ which is produced by marine biogenic activity and is the dominant source of sulfate aerosol ~~,~~

5 ~~change~~ over the Southern Ocean~~when the chlorophyll-a distribution, which influences oceanic DMS production , is altered. Using a nudged~~. However, DMS production is poorly constrained in Earth system models. Using an atmosphere-only nudged to observations configuration of the ~~atmosphere-only~~ United Kingdom Earth System Model ~~,~~(UKESM1-AMIP), we performed ~~nine~~ eight 10-year simulations ~~using forcings representative of the period 2009 − 2018. Four different~~ for the recent past (2009–2018). We tested four seawater DMS data sets ~~are tested as input for these simulations. Three different~~ and three DMS

10 sea-to-air ~~flux parameterizationsare also explored. Our goal is to evaluate the changes in~~ transfer velocity parameterizations. All data sets and parameterizations are commonly used by present-day Earth system models, with the exception of one data set that we developed from satellite chlorophyll-a data. We evaluate simulated oceanic DMS, sea-to-air ~~fluxes~~ transfer of DMS, and atmospheric DMS ~~through these different simulations~~ during austral summer. ~~The mean spread across all the~~ In simulations with different ~~oceanic DMS datasets,~~ seawater DMS data sets but the same sea-to-air flux ~~parameterizations, is~~

15 parameterization, Southern Ocean summertime DMS varies by 112% (3.3 to 6.9 TgS Yr^{-1}). ~~The mean spread in~~ This is approximately twice as much as the simulations using the same ~~oceanic DMS dataset,~~ seawater DMS data set but differing sea-to-air flux ~~parameterisations is~~ parameterizations, in which DMS varies by 50-60% (2.9 to 4.7 TgS Yr^{-1}). The choice of ~~DMS emission parameterisation~~ oceanic DMS source has a larger influence on atmospheric DMS than the choice of ~~oceanic DMS source. We also find that linear relationships between wind and DMS flux generally compare better to observations than~~ DMS

20 emission. Simulations testing different sea-to-air transfer velocity parameterizations show that simulating a linear dependence of DMS gas transfer velocity as a function of wind speed results in a more accurate representation of atmospheric DMS

distributions than using quadratic relationships. Simulations ~~that implement a quadratic emission rate show on average 35% higher DMS mixing ratios than the linear emission rates. Simulations~~ using seawater DMS derived from satellite ~~chlorophyll-a data in combination with a recently-developed flux parameterisation for DMSshow the closest~~ chlorophyll-a data show realistic spatiotemporal variability in DMS and when combined with a recently developed transfer velocity parameterization for DMS, the model shows good agreement with atmospheric DMS observations~~and are recommended to be included in future simulations~~. As a precursor for natural sulfate aerosol and cloud condensation nuclei, DMS plays an important role in the radiative balance over the Southern Ocean. This work ~~recommends for Earth System Models to include a~~ highlights that the seawater DMS data sets and sea-to-air transfer velocity parameterizations for DMS commonly used in climate models are poorly constrained for the Southern Ocean region. We recommend that models use a DMS sea-to-air parameterization that ~~is appropriate~~ was developed specifically for DMS, and for oceanic DMS datasets to ~~include inter-annual~~ incorporate spatial variability based on observed marine biogenic activity. Such improvements will provide a more accurate process-based representation of oceanic and atmospheric DMS, and therefore sulfate aerosol, in the Southern Ocean region.

1 Introduction

The representation of aerosols over the Southern Ocean is a large source of uncertainty in climate models due to the lack of observational data and large seasonal variability (Revell et al., 2019). Poor representation of aerosols contributes to the large biases in future climate projections over the Southern Ocean (Myhre et al., 2014). Sea spray and dimethyl sulfide (DMS; CH_3SCH_3) are fundamental sources for aerosol formation over this region (Revell et al., 2021; Bhatti et al., 2022). The dominant source of sulfate over the marine atmosphere is the biogenic marine aerosol precursor DMS, controlled by ~~phytoplankton productivity (Keller et al., 1989; Bates et al., 1987; Berndt et al., 2019)~~marine biota (Keller et al., 1989; Bates et al., 1987; Kiene and Bates, 1990; Curs. Revell et al. (2019) found sulfate aerosol production from DMS was responsible for around 60% of the austral summer aerosol optical depth over the Southern Ocean. Atmospheric DMS therefore has the potential to greatly influence cloud condensation nuclei during austral summer ~~, due to its high rate of emissions~~ (Kloster et al., 2006; Revell et al., 2019; Korhonen et al., 2008; Pandis et al., 1994).

The Southern Ocean contains extremely high phytoplankton and marine biota productivity during austral summer (~~December, January, and February~~DJF, December–February) (Deppeler and Davidson, 2017). ~~Phytoplankton~~Marine biogenic activity plays a key role in chlorophyll-a (chl-a) production and is considered to be a key driver of oceanic DMS production (e.g. Uhlig et al., 2019; Townsend and Keller, 1996; Anderson et al., 2001; Deppeler and Davidson, 2017). Earth System Models (ESMs) represent the process of oceanic DMS formation through multiple ~~mechanisms, with varying focus~~approaches that are dependent on chl-a, nutrients, light, mixed-layer depth, zooplankton, and dimethylsulfoniopropionate concentration (Bock et al., 2021). The UKESM1 and MIROC-ES2L models use a diagnostic approach to represent chl-a (Sellar et al., 2019; Anderson et al., 2001; Hajima et al., 2020). The CNRM-ESM2-1 and NorESM2-LM ~~focus on~~ models use a prognostic approach, closely related to zooplankton and dimethylsulfoniopropionate ~~,~~abundance, which are both precursors of oceanic DMS (Seland et al., 2020; Séférian et al., 2019). Bock et al. (2021) evaluated oceanic DMS in CMIP6 models ~~simulate biases in oceanic DMS production~~

55 ~~compared~~ and found that all models are biased in comparison with observational climatologies of DMS in the Southern Ocean region ~~(Bock et al., 2021).~~

Atmosphere-only global climate models use climatologies to ~~approximate~~ prescribe the global concentration of oceanic DMS. Lana et al. (2011) and Kettle et al. (1999) constructed observational climatologies of oceanic DMS which are used ~~within climate~~ by such models. However, there is a limited amount of data available within the Southern Ocean, which can

60 lead to ~~biases when compared to other regions~~ errors in the representation of oceanic DMS (e.g. Bock et al., 2021; Mulcahy et al., 2020). A limitation of representing oceanic DMS as a static climatology is that it does not account for the large temporal variations in DMS concentrations observed. For instance, El Niño Southern Oscillation (ENSO) events, wildfires, and volcanic eruptions all significantly influence oceanic DMS within the Southern Ocean (e.g. Yoder and Kennelly, 2003; Tang et al., 2021; Wang et al., 2022; Browning et al., 2015; Longman et al., 2022). Calculating oceanic DMS online using a biological proxy

65 would resolve these perturbing events to some degree (Galí et al., 2018).

~~DMS is emitted~~ The flux of DMS from the ocean to the atmosphere ~~and has a strong dependence on the~~ depends on the gas transfer velocity, which in turn depends on the surface wind speed ~~(e.g. Fairall et al., 2011). A wealth of research has focused on better understanding the relationship between atmospheric DMS and wind speed (Vlahos and Monahan, 2009; Zavarsky et al., 2018; Blom~~ ~~. However, the uncertainty in this relationship remains high particularly within the Southern Ocean due to a lack of observational~~

70 ~~data (e.g. Elliott, 2009; Smith et al., 2018; Zhang et al., 2020), particularly for wind speeds $\geq 13\,\mathrm{ms}^{-1}$ (Blomquist et al., 2017)~~ ~~. Recently, significant progress has been made as recent literature has established that DMS flux has a linear relationship with wind (Goddijn-Murphy et al., 2016; Blomquist et al., 2017; Bell et al., 2015), while Earth System Models continue to use older quadratic relationships to represent DMS emissions Bock et al. (2021)~~ (e.g. Fairall et al., 2011). Many DMS flux parameterizations have been developed, but most use transfer velocities measured for gases other than DMS (Wanninkhof, 1992, 2014; Nigh

75 . Some studies, including Blomquist et al. (2017) and Yang et al. (2011), used DMS measurements to derive a relationship between wind speed and DMS. Depending on the solubility of the gas measured, gas transfer velocities typically have a linear or quadratic dependence on wind speed. Linear relationships best represent gases with intermediate solubilities, such as DMS (e.g. Blomquist et al., 2017; Goddijn-Murphy et al., 2016; Bell et al., 2015; Yang et al., 2011; Huebert et al., 2010), while quadratic equations are better suited for highly soluble gases like CO_2 (Wanninkhof, 2014; Nightingale et al., 2000; Wanninkhof, 1992).

80 ~~Oceanic DMS observations~~ Uncertainty in DMS emissions remains high, particularly in the Southern Ocean ~~are highly variable in time and space (Lana et al., 2011; Hulswar et al., 2022; Galí et al., 2018), while the emissions of DMS are also uncertain (e.g. Korhonen et al., 2008; Blomquist et al., 2017). This study sets out to examine whether including oceanic DMS with spatio-temporal variabilitybased on real-world~~ region where wind speeds are high and observational data sparse (e.g. Elliott, 2009; Smi ~~. ESMs use a variety of transfer velocities to represent DMS emissions (Bock et al., 2021). UKESM1 uses the Liss and Merlivat (1986)~~

85 parameterization even though it was constructed for gases other than DMS.

Here we examine whether incorporating realistic oceanic DMS variability, based on remotely-sensed chl-a observations improves the simulation of atmospheric DMS. ~~We investigate differences in oceanic DMS and emission parameterizations for forming atmospheric DMS using the nudged to observation configuration of~~ Using a nudged configuration of the atmosphere-only United Kingdom Earth System Model (UKESM1-AMIP ~~. We calculate~~), we use three established oceanic DMS datasets

90 and three transfer velocity parameterizations. We also test a 10-year monthly time series ~~calculated from chl-a~~ in which seawater DMS is calculated offline from MODIS-aqua satellite ~~data implemented within the modified Anderson et al. (2001) parameterization (Sellar et al., 2019). We also test climatologies from Lana et al. (2011), Hulswar et al. (2022), and the DMS climatology used by UKESM1-AMIP (Sellar et al., 2019).~~ chl-a data using the Anderson et al. (2001) oceanic DMS parameterization which is used by UKESM1 (Sellar et al., 2019). We evaluate sea-to-air fluxes of DMS and oceanic and atmospheric DMS

95 concentrations relative to station and ship-based observations. The observational data sets are described in Section 2.4, the model configuration is described in Section 2.1, and details of the oceanic DMS ~~emissions are calculated using two quadratic (Wanninkhof, 2014; Nightingale et al., 2000) and two linear (Liss and Merlivat, 1986; Blomquist et al., 2017)~~ data sets and sea-to-air ~~flux parameterizations. Evaluating the process and sensitivity of DMS from the ocean to the atmosphere in climate models is critical for the further development of models and for understanding the biogeochemical cycle. We compare the DMS~~

100 ~~variability across the Southern Ocean during summer, improving our understanding of the relative importance of choosing the source (oceanic DMS) and emissions.~~ transfer velocity parameterizations tested are in Sections 2.2 and 2.3, respectively. Results follow in Section 3.

2 Methods

2.1 Model Configuration and Evaluation

105 Simulations were performed using the atmosphere-only configuration of the coupled UK Earth System Model (UKESM1; Yool et al., 2020; Sellar et al., 2019; Mulcahy et al., 2020). By default, atmospheric DMS is produced via the Lana et al. (2011) oceanic DMS data set and Liss and Merlivat (1986) sea-to-air transfer velocity parameterization. Atmospheric DMS then oxidises to form sulfate aerosols. In UKESM1~~simulates ocean biogeochemistry via an intermediate complexity biogeochemical dynamic model, MEDUSA2.0 (the Model of Ecosystem Dynamics, nutrient Utilization, Sequestration, and Acidification; Yool et al., 2020~~

110 ~~. MEDUSA is used in UKESM1 to represent biogeochemical feedbacks within the Nucleus for European Modelling of the Ocean (NEMO) ocean model (Madec and others, 2008). The aerosol component of UKESM1 uses the GLOMAP-mode aerosol scheme, which is described in full by Mulcahy et al. (2020) and Mann et al. (2010, 2012).~~ aerosol growth, chemistry and removal are handled by the GLOMAP-mode scheme (Mulcahy et al., 2020).

Wind and temperatures ~~within the simulations used in this study are nudged 6-hourly to real-world conditions via the~~

115 ~~use of the~~ are nudged to 6-hourly ERA-5 reanalysis data (Hersbach et al., 2020). The full description of ~~how nudging is incorporated within the UKESM1-AMIP is outlined in more detail by Telford et al. (2008). As noted by Pithan et al. (2022) and Kuma et al. (2020), nudging simulations can enhance the precision of simulations used for assessing atmospheric processes. Specifically, it allows for a more accurate representation of meteorological factors such as wind speed, which play a key role in~~ the nudging configuration is outlined in Telford et al. (2008). Nudging ensures that wind speeds, which are pivotal to the

120 formation of atmospheric DMS. ~~Using nudged runs also allows us to better evaluate our simulations against observational measurements made during voyages.~~

~~The sea-to-air transfer of DMS in our simulations is discussed in Section 2.3. All simulations in this study~~, are accurately represented (Pithan et al., 2022; Kuma et al., 2020) and allows like-for-like comparisons against observations. Sea surface temperature and sea ice data from The Hadley Centre Global Sea Ice and Sea Surface Temperature were used (HadISST; Titchner and Rayner, 2014). Simulations are 10 years long, spanning from 2009 to 2018. ~~We focus on the austral summer months (December–February; DJF)due to the summer being the most biologically productive season~~ This period was chosen to coincide with the availability of recent DMS observations (Section 2.4).

~~In this paper, we compare observational data to our simulations using the same hourly timescales~~Atmospheric DMS concentrations are analyzed at the lowest model level, at 20 m during DJF, which is the most productive season for DMS (Deppeler and Davidson, 2017; Jar. Hourly output was saved to compare with observations where applicable (for example, voyages provide observations at hourly temporal frequency). To evaluate variability, we use the coefficient of variation (CoV)~~which is a statistical measure that compares the variability of data by expressing the standard deviation as a percentage of the mean. CoV is used to compare the variability between each of the simulations oceanic DMS, DMS emissions, and atmospheric DMS concentration.~~. A higher CoV suggests that the variability or dispersion of the data is relatively large compared to its mean. Where uncertainty is reported, ~~1 standard deviation through time and space~~ one standard deviation calculated over the relevant domain and time period is stated.

2.2 Oceanic DMS

We input four oceanic DMS data sets into the ~~atmospheric~~ model: three climatologies and one 10-year ~~time-series between 2009 to 2018. Two are observational-based climatologies~~ time series. Observational-based climatologies are from Lana et al. (2011) (hereafter 'Lana') and Hulswar et al. (2022) (~~hereafter~~ 'Hulswar'). The 'MEDUSA' climatology (1979-2014) ~~is sourced~~ originates from the UKESM1 CMIP6 ~~repository, MEDUSA (Yool et al., 2021; Sellar et al., 2019). See~~ (Yool et al., 2021; Sellar et al., 2019. Table 1 ~~for an outline of~~ outlines the oceanic DMS ~~climatologies and dataset used.~~ datasets used. Ocean biogeochemistry is simulated in the UKESM1 via MEDUSA2.0 (the Model of Ecosystem Dynamics, nutrient Utilization, Sequestration, and Acidification; Yo. The time series was calculated offline using a combination of satellite data and the UKESM1 approach to calculating seawater DMS, as described below.

~~The~~ In UKESM1~~uses a diagnostic approach in the formulation of oceanic DMS, which is calculated online using~~, oceanic DMS concentrations are calculated using a diagnostic method from Anderson et al. (2001), using surface daily shortwave radiation (J), dissolved inorganic nitrogen (Q), and ~~surface~~ chl-a (C):

$$Oceanic\ DMS = a,\ for\ log(CJQ) \leq s \tag{1}$$

$$Oceanic\ DMS = b[log(CJQ) - s] + 1,\ for\ log(CJQ) > s \tag{2}$$

The ~~fitted~~ parameter values are a=1, b=8, and s=1.56, as described by Sellar et al. (2019). ~~The online oceanic DMS from MEDUSA in the UKESM1 shows small annual variability and therefore a 30-year climatology will represent MEDUSA~~

Table 1. Oceanic DMS data sets used in the model simulations.

Oceanic DMS dataset	Source	Citation	Year of Data
Lana	Oceanic DMS observations	Lana et al. (2011)	1972 - 2009
Hulswar	Oceanic DMS observations	Hulswar et al. (2022)	1972 - 2021
MEDUSA	UKESM1 CMIP6 simulations	Anderson et al. (2001); Sellar et al. (2019)	1979 - 2014
MODIS-DMS	MODIS-aqua chlorophyll-a via Anderson et al. (2001)	N/A (produced for this study)	2009 - 2018

well. Q and , chl-a are taken from MEDUSA, and J is from the atmosphere component of the UKESM1, the Unified Model. Chl-a is used to calculate oceanic DMS concentrations in other are averaged from CMIP6 models, such as MIROC-ES2L, and within algorithms such as that detailed by Galí et al. (2018). The Anderson et al. (2001) parameterization is a widely used for the MEDUSA climatology. The Anderson et al. (2001) parameterization produces positive biases in DMS over the Southern Ocean within MEDUSA (Bock et al., 2021) due to the set minimum oceanic concentration of 1, which leads to large average DMS concentrations (Yool et al., 2021; Bock et al., 2021). Recent research suggests that chl-a may not be an appropriate proxy for oceanic DMS (Uhlig et al., 2019; Bell et al., 2021), and well-validated method for calculating oceanic DMS in UKESM1. Here, we have tested a modified version of it using the MODIS-aqua future work will explore alternative methods for calculating oceanic DMS within UKESM1. Nonetheless, chl-a is widely used by CMIP6-era models to calculate oceanic DMS, and we explore here whether using an observationally derived chl-a dataset. This data set, concentration field leads to changes in the spatial and temporal variability of atmospheric DMS. Monthly-mean chl-a concentrations from the Moderate Resolution Imaging Spectroradiometer (MODIS)-aqua satellite instrument were used to construct a time series of oceanic DMS between 2009–2018 (Table 1; Hu et al., 2019; O'Reilly and Werdell, 2019). This time series, which we term the 'MODIS-DMS' , is a continuous time series between 2009 to 2018. MODIS-DMS is data set, is calculated offline using the same diagnostic parameterization (Anderson et al., 2001; Sellar et al., 2019) as Equations 1 and 2. The UKESM1 has a +6 W m^{-2} bias for J within CMIP6 over the Southern Ocean, which may result in slightly higher oceanic DMS concentrations (Schuddeboom and McDonald, 2021). The J and Q used to calculate MODIS-DMS remain the same to MEDUSA, but a new monthly-mean as MEDUSA. Through this, we capture spatial and interannual chl-a field (C) is introduced via Moderate Resolution Imaging Spectroradiometer (MODIS) -Aqua Level-3 ocean-color chl-a (Table 1; e.g. Hu et al., 2019; O'Reilly and Werdell, 20 variability, indicating biological productivity. Bi-linear interpolation is used to fill in small gaps (around 1% for monthly averages) of spatial chl-a data. Using the MODIS-Aqua chl-a satellite data, oceanic DMS concentrations were calculated each month for our 10 year period. From this, we capture the annual variability of the distribution in ocean biological productivity (referenced in this work as MODIS-DMS). Our goal is to understand the relationship between oceanic biological productivity, as represented by chl-a, and atmospheric DMS concentrations in the Southern Ocean during austral summer. We then evaluate which oceanic DMS sources produce the best distribution compared to observations. Oceanic DMS concentrations are masked where they coincide within the sea-ice zone from HadISST.

180 ~~Several studies have validated the~~ In general, the MODIS-aqua Ocean Color chl-a retrieval ~~, finding it to generally underestimate Southern Ocean conditions (Zeng et al., 2016; Haëntjens et al., 2017; Jena, 2017). Satellites can also overestimate chl-a measurements due to the scattering of light from aerosols (Schollaert et al., 2003). However, Marrari et al. (2006) found satellite chl-a is accurate within the Southern Ocean during summer. Therefore the~~ underestimates Southern Ocean chlorophyll concentrations (Zeng et al., 2016; Haëntjens et al., 2017; Jena, 2017; Gregg and Casey, 2007; Johnson et al., 2013). Simulated oceanic DMS

185 may therefore be systematically underestimated. Nonetheless, the high spatial and temporal availability of ~~summertime data makes~~ chl-a ~~a viable option for estimating phytoplankton productivity and oceanic DMS. Using the MODIS-DMS data set, we aim to accurately simulate maxima and minima in oceanic DMS concentrations comparable to observations. By comparing the model results with observations, we can identify and understand the impact of phytoplankton bloom events and annual variability which can not be captured by climatologies.~~ observations during summertime makes it useful to explore spatiotemporal

190 variability in atmospheric DMS.

2.3 DMS Sea-to-Air Flux

~~To calculate the transfer of DMS from the ocean to the atmosphere, a parameterization is used which is controlled by wind speed. The formulation of the transfer velocity is derived from observational measurements of a particular gas. Many flux parameterisations have been developed, but these have mostly been based on gases such as CO_2 (e.g. Wanninkhof, 2014). These~~

195 ~~parameterizations are widely implemented within climate models to represent DMS but vary depending on the model. We tested three flux parameterisations shown in~~ Three DMS transfer velocities are tested (Figure 1~~. Blomquist et al. (2017) (hereafter 'B17') used DMS measurements to derive a relationship between wind speed and DMS, whereas Wanninkhof (2014) (W14) and Liss and Merlivat (1986) (~~, Table 2). Two are linear equations from Liss and Merlivat (1986) (hereafter 'LM86~~) used CO_2, and other high solubility gases. Sea-to-air parameterizations are typically linear or quadratic, depending on the solubility of the gas.~~

200 ~~Linear equations best represent gases with intermediate solubilities, such as DMS (e.g. Blomquist et al., 2017; Goddijn-Murphy et al., 2016, while quadratic equations are better suited for highly soluble gases like CO_2 (Wanninkhof, 2014; Nightingale et al., 2000; Wanninkhof, 19. This study uses two linear equations from LM86 and~~') and Blomquist et al. (2017) (hereafter 'B17~~to represent DMS emissions more accurately compared with observations, as suggested by Blomquist et al. (2017) and Goddijn-Murphy et al. (2016). LM86 is a piecewise function consisting of three lines with different gradients and intercepts, depending on the wind speed (Figure 1~~').

205 LM86 is ~~used as the default flux parameterization within~~ the default parameterization within UKESM1 (Sellar et al., 2019) and ~~is thus used on with oceanic DMS datasets~~was evaluated in combination with all oceanic DMS data sets. The quadratic formula from Wanninkhof (2014) (hereafter 'W14') is also tested. Using these different parameterizations provides an ~~estimate of~~ appropriate estimate for the spread of DMS emissions ~~. The Lana oceanic DMS climatology is tested with the W14, and B17 fluxes, as Lana is currently the most widely used climatology within climate models (Bhatti et al., 2022). We also apply~~

210 ~~the W14 and B17 flux parameterisations to the MODIS-DMS oceanic DMS dataset to test the~~ due to the upper and lower limits of ~~oceanic DMS concentrations to assess the variation from the time-series~~DMS transfer velocity tested from in-situ DMS measurements (e.g. Goddijn-Murphy et al., 2016; Blomquist et al., 2017). Table 2 ~~outlines the sensitivity simulations performed~~for this study, described by summarizes the sensitivity simulation names performed. Simulations are named with the

Table 2. Simulations used in this study, ~~named~~ with the oceanic DMS ~~data sets as the name~~concentration used, ~~followed by~~ subscripted with the ~~DMS flux parameterization~~ sea-to-air transfer velocity used.

Simulation name	Oceanic DMS source	DMS ~~flux~~ transfer velocity parameterization
Lana$_{LM86}$	Lana et al. (2011)	Liss and Merlivat (1986)
Lana$_{B17}$	Lana et al. (2011)	Blomquist et al. (2017)
Lana$_{W14}$	Lana et al. (2011)	Wanninkhof (2014)
Hulswar$_{LM86}$	Hulswar et al. (2022)	Liss and Merlivat (1986)
MEDUSA$_{LM86}$	Anderson et al. (2001); Sellar et al. (2019)	Liss and Merlivat (1986)
MODIS$_{LM86}$	N/A (produced for this study)	Liss and Merlivat (1986)
MODIS$_{B17}$	N/A (produced for this study)	Blomquist et al. (2017)
MODIS$_{W14}$	N/A (produced for this study)	Wanninkhof (2014)
MODIS$_{B17}$CLIM	N/A (climatology produced for this study)	Blomquist et al. (2017)

oceanic DMS concentration used, subscripted with the sea-to-air ~~flux~~ transfer velocity used. For example, Lana$_{LM86}$ means

215   that the simulation used the Lana et al. (2011) climatology as its oceanic DMS source, and the DMS ~~flux parameterisation~~ transfer velocity parameterization of Liss and Merlivat (1986).

~~To calculate the flux of DMS, the Schmidt number of DMS is required~~The Schmidt number for DMS is used to calculate the DMS emission. The Schmidt number ~~describes the mixing efficiency of a substance in a fluid and is used to calculate the transfer velocity of gas~~from the sea to air~~represents the viscosity/diffusion properties of a gas, varying with respect to sea

220   surface temperature (T in °C). We update the Schmidt number of DMS (Sc_{DMS}) used in the UKESM1 from the formulation used in Saltzman et al. (1993) to Wanninkhof (2014), as shown in Equation 3:

$$Sc_{DMS} = 2855.7 + (-177.63 + (6.0438 + (-0.11645 + 0.00094743 \cdot T) \cdot T) \cdot T) \cdot T \qquad (3)$$

~~T is the sea surface temperature derived from The Hadley Centre Global Sea Ice and Sea Surface Temperature (HadISST) within the model (Titchner and Rayner, 2014). LM86 was constructed based on gases other than DMS, but is often used for~~

225   ~~DMS emissions within CMIP6 Earth System and climate models (e.g. Horowitz et al., 2020; Tang et al., 2019; Yukimoto et al., 2019). In equation 4,~~ Where T is derived from HadISST (Titchner and Rayner, 2014). U_{10} ~~is the wind speed at~~ (m s^{-1}) represents near-surface (10~~m above the surface~~ m) wind speed and K_w (cm h^{-1}) represents the transfer velocity of DMS. Equation 4 represents the LM86 transfer velocity of DMS:

for $u_{10} \leq 3.6$:

$$K_w = 0.17 \left(\frac{600}{Sc_{DMS}} \right)^{\frac{2}{3}} u_{10},$$

for $3.6 \leq u_{10} < 13$:

$$K_w = 2.85 \left(\frac{600}{Sc_{DMS}} \right)^{\frac{1}{2}} (u_{10} - 3.6) + 0.612 \left(\frac{600}{Sc_{DMS}} \right)^{\frac{2}{3}},$$

for $u_{10} > 13$:

$$K_w = 5.9(u_{10} - 13) \left(\frac{600}{Sc_{DMS}} \right)^{\frac{1}{2}} + 26.79(u_{10} - 3.6) \left(\frac{600}{Sc_{DMS}} \right)^{\frac{1}{2}} + 0.612 \left(\frac{600}{Sc_{DMS}} \right)^{\frac{2}{3}} \tag{4}$$

W14 uses a quadratic formula (equation 5) ~~to empirically fit observations of CO₂ as a~~ for sea-to-air transfer. W14 is also ~~very frequently~~ used to calculate DMS emissions amongst CMIP6 ~~simulations~~ models (e.g. Tjiputra et al., 2020).

$$K_w = 0.251 \cdot u_{10}^2 \left(\frac{660}{Sc_{DMS}} \right)^{\frac{1}{2}} \tag{5}$$

~~Finally,~~ B17 is the only parameterization ~~used~~ tested in this study ~~which calculates a transfer velocity~~ for which the transfer velocity is based on real-world observation of DMS (~~equation~~Equation 6). B17 is a superlinear ~~and sub-quadratic~~ parameterization, however, for simplicity and the wind speeds used in this study, we label B17 as a linear parameterization.

$$K_w = 0.7432 \cdot u_{10}^{1.33} \left(\frac{660}{Sc_{DMS}} \right)^{\frac{1}{2}} \tag{6}$$

To assess the inter-annual variability of DMS emissions and atmospheric DMS concentrations, we performed an additional 10-year simulation, MODIS$_{B17}$CLIM. While MODIS$_{B17}$ used a 10-year time series of oceanic DMS derived from MODIS chlorophyll-a data, MODIS$_{B17}$CLIM used a climatology calculated from monthly-mean data for the 10-year MODIS$_{B17}$ time series.

2.4 Observational Datasets

2.4.1 DMS Datasets

Two Southern Ocean voyages are used to ~~validate~~ evaluate our simulations: the SOAP ~~(Surface Ocean Aerosol Production; Bell et al., 2015)~~ ~~campaign~~ campaign (Surface Ocean Aerosol Production; Bell et al., 2015; Law et al., 2017) and RV Tangaroa voyage (TAN1802; Kremser et al., 2021). The SOAP voyage measured oceanic and atmospheric DMS from Feb-March 2012 near the Chatham Rise (within 42–47 °S, 172–180 °E) off the east coast of New Zealand ~~, a highly biologically productive region of the Southern Ocean~~ (Bell et al., 2015; Smith et al., 2018). The TAN1802 voyage measured oceanic DMS along ~~a transect in~~ the Southern
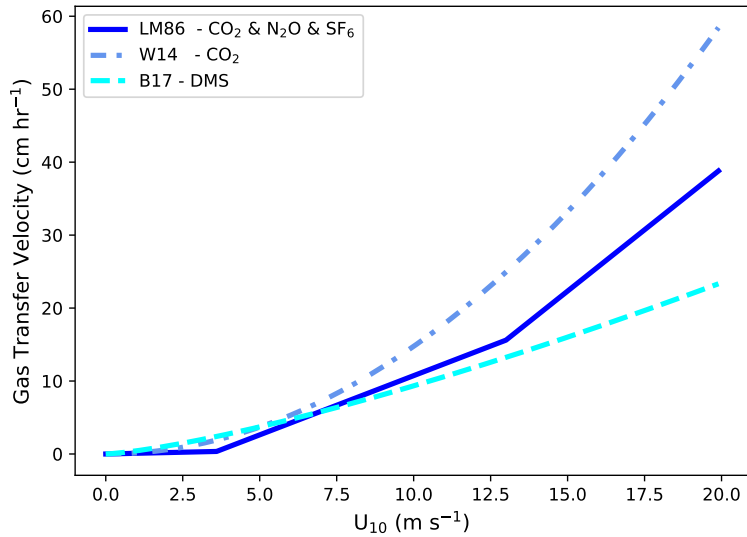
Figure 1. DMS ~~sea-to-air flux parameterizations~~ transfer velocities tested in this study. LM86 = Liss and Merlivat (1986); W14 = Wanninkhof (2014)~~and~~; B17 ~~represents~~ = Blomquist et al. (2017). The gases labelled in the legend are the measurements taken to identify the gas exchange relationship.

Ocean during Feb-March 2018 between ~~latitudes~~ 40 °S to 70 °S, 180 °E (Kremser et al., 2021). ~~Other voyages outside the~~ ~~years covered by our nudged simulations , but included in the atmospheric DMS analysis are the SOIREE and ANDREXII~~

250 ~~voyages, used to calculate the observational atmospheric DMS . SOIREE occurred in~~ We also extend the simulations to cover the ANDREXII voyage between Feb - April 2019 for atmospheric DMS concentrations as this voyage mostly measured during autumn (Wohl et al., 2020). ANDREXII traveled longitudinally around 60 °S. Although outside our simulation range, we also consider SOIREE for atmospheric DMS analysis from Feb 1999 ~~and measured atmospheric DMS concentration~~ (Boyd and Law, 2001) between 42 - 63 °S, 139–172 °E. ~~ANDREXII (Wohl et al., 2020) travelled longitudinally around 60 °S, between~~

255 ~~February to April 2019.~~

We used oceanic DMS measurements for TAN1802 Kremser et al. (2021), SOAP (Bell et al., 2015), and ERA-5 surface wind speeds (Hersbach et al., 2020) to calculate hourly DMS emissions. The ~~Wanninkhof (2014)~~ Wanninkhof (2014) DMS Schmidt number is calculated using the same parameters used within the simulations, for consistency with comparisons to simulated fluxes. ~~Sea ice and sea surface temperature data are from the Met Office Hadley Centre's sea ice and sea surface temperature~~

260 ~~(HadISST; Titchner and Rayner, 2014), where sea surface temperature represents T in Equation 3.~~ The HadISST and ERA-5 wind speed data were obtained for the same time and location as the two voyages (within the nearest ~~neighbour~~ neighbor grid cell). We applied three different sea-to-air flux parameterizations (LM86, B17, and W14) to both SOAP and TAN1802 voyage paths (See section 3.2).

We compare our simulations to the voyage dataset using the hourly model output and identify the nearest ~~neighbour~~ neighbor
grid cell to the ship location. Analysis of oceanic DMS data used in the models is also synchronized to TAN1802 and SOAP
voyages, using the same timescales for comparing the voyages with model data.

We also validate the model using atmospheric DMS concentrations measured at ~~three~~ two stations: Cape Grim (1989 to
1996; 41 °S and 145 °E) ~~; Amsterdam Island (1987 to 2008; 38 °S, 78 °E);~~ and King Sejong Station (2018 to 2020; 62 °S,
58 °W). King Sejong is located on the Antarctic Peninsula, where sea ice melt occurs during our study period, which can
profoundly increase DMS emissions, as previously found by Berresheim et al. (1998); Read et al. (2008). ~~The climatologies
from Amsterdam Island and Cape Grim stations~~

2.4.2 Cloud and Aerosol Observations

MODIS-aqua aerosol optical depth (AOD) measurements at 550 nm (Platnick et al., 2017) are compared with ~~the model
climatology of atmospheric DMS. The King Sejong measurements align with our simulation period, and so we compare both
datasets~~ ~~on the same timescale~~ each daily-mean model output. Daily-averaged observations from Grosvenor et al. (2018) and
Bennartz and Rausch (2017) were used to compare the cloud droplet number concentration (CDNC) with our daily-averaged
simulations. Finally, to evaluate cloud condensation nuclei (CCN), we used Choudhury and Tesche (2023) at 818 m, in comparison
with simulated CCN at 800 m. The description and evaluation of using MODIS-observed AOD compared with a related
configuration of UKESM1-AMIP is discussed in more detail in Revell et al. (2019) and Mulcahy et al. (2020). We calculate an
austral summertime climatology for these observational datasets, which we use over the Southern Ocean.

3 Results and Discussion

3.1 Oceanic DMS

Figure 2a-d shows the spatial distribution of ~~the oceanic DMS from the different datasets used in this study~~each oceanic
DMS dataset. Each distribution has key defining characteristics, although Hulswar (Figure 2d) is ~~similar~~ an update to Lana
(Figure 2c)~~as it is an updated version. When the dataset includes chlorophyll-a (chl-a), oceanic DMS has distinguishable
features across latitudes, partly due to the influence of the Southern Hemisphere westerly jet, driving ocean circulation and
transporting phytoplankton (e.g. Allison et al., 2010; Li et al., 2016). The only difference between the calculation of~~ . The
distinction between MODIS-DMS and MEDUSA oceanic DMS ~~is the~~ calculations is chl-a~~input, however, their distributions
of oceanic DMS in the Southern Ocean are largely different~~ , ~~as illustrated~~ which results in distinctly different distributions,
as shown in Figure 2e. Observational-based climatologies, ~~such as in~~ like Lana or Hulswar~~(Figure 2c, d), do not consider
other proxies of oceanic DMS (Lana et al., 2011; Hulswar et al., 2022). Lana and Hulswar (Figure 2c,d), do not match the
distribution of~~ , do not align with the chl-a distribution in the Southern Ocean, particularly along the Antarctic Circumpolar
Current, ~~as oceanic DMS concentrations are focused to a specific region,~~ concentrating oceanic DMS in specific regions based
only on observations of oceanic DMS (Lana et al., 2011; Hulswar et al., 2022). The mean difference between the ~~mean of~~

~~MODIS and MEDUSA (the lowest and highest~~ lowest (MODIS-DMS) and highest (MEDUSA) mean of all the oceanic DMS datasets used ~~)~~is 107%~~, respectively~~.

MEDUSA produces the most homogeneous oceanic DMS distribution in the summertime Southern Ocean, with the highest mean ~~of 4.88 nM. Additionally, it has the~~ and smallest standard deviation ~~of~~ (4.88±0.87 nM~~(and~~). It also has the lowest CoV of ±17% indicating a small spread of variance). ~~The chl-~~. Chl-a ~~calculated by MEDUSA has~~ in MEDUSA shows a positive bias ~~when compared to~~ against summer observations in the Southern Ocean ~~during summer (Yool et al., 2013, 2021), resulting in higher oceanic DMS concentrations than other datasets~~(Yool et al., 2013, 2021). In contrast, ~~the~~ MODIS-DMS ~~dataset produces~~ has low oceanic DMS concentrations in open ocean regions, ~~but very~~ and high concentrations in biologically productive regions (near the subtropical front), such as the Chatham Rise and coastal South America (Behrens and Bostock, 2023). MODIS-DMS ~~exhibits large variability due to locally-enhanced chl-a concentrations along coastal regions and the mid-latitudes (40-50 °S)of the Southern Ocean. Oceanic DMS from MODIS has a mean of~~ has the largest spatial variability in oceanic DMS overall (CoV 67%). The mean oceanic DMS in MODIS-DMS is 2.36±1.57 nM~~(CoV of 67%)~~, which is outside the range of ~~oceanic DMS produced by~~ MEDUSA, highlighting the sensitivity of the Anderson et al. (2001) parameterization to ~~the~~ chl-a ~~concentration~~concentrations.

In the MODIS-DMS simulation, oceanic DMS concentrations vary each ~~summertime~~ summer across the Southern Ocean ~~during the 10 year~~ over a 10-year climatology (See Figure ~~?? in the supplementary materials~~??a in the appendix). The ~~year with the highest mean oceanic DMS concentration observed by the MODIS-DMS dataset (2.58±2.12 nM) occurred in 2010 (Figure ??), with a 16.2% higher concentration than the lowest concentration in 2015 (2.22±1.88 nM). The largest interannual variability in MODIS-DMS~~ most significant interannual variability occurs around New Zealand and ~~the East Coast of South Americaand is likely caused by specific phytoplankton bloom events, possibly being~~ South America's East Coast, likely from phytoplankton blooms influenced by ENSO (e.g. Santoso et al., 2017; Thompson et al., 2015; Yoder and Kennelly, 2003)~~. Oceanic DMS climatologies do not capture these inter-annual oceanic events. Furthermore, voyages that measure oceanic DMS often have specific research targets which can cause asampling bias within the climatologies compiled from in-situ observations. Voyages also only collect data during specific months within specific regions. For example, the SOAP voyage targeted phytoplankton blooms and their accompanying high oceanic DMS concentrations (Bell et al., 2015).~~

~~Factors such as melting sea ice can also affect chl-a, and therefore oceanic DMS (Behera et al., 2020; Berresheim et al., 1998). Phytoplankton activity, such as bloom events, affect chl-a concentrations (e.g. Uhlig et al., 2019; Matrai et al., 1993) and will be captured by the MODIS-DMS simulations, but not by the climatologies; MEDUSA currently lacks the ability to represent realistic phytoplankton blooms in chl-a concentrations (Yool et al., 2021).~~

(Figure 2a). The Lana and Hulswar simulations have similar means ~~and CoV, respectively, across the entire Southern Ocean during austral summer~~ (3.87 nM and 3.51 nM~~; CoV of 31% and 32%). However, the distribution of both datasets~~, respectively) but differ in their distribution (Figure 2e)~~is different: Lana contains much higher concentrations, maximizing~~. Oceanic DMS maximises at 30 nM ~~compared to~~ in Lana, and at 14 nM ~~from Hulswar. Using~~ in Hulswar. The MEDUSA simulation using the Anderson et al. (2001) parameterization ~~while changing the chl-a input, MEDUSA calculates a peak DMS concentration~~ shows oceanic DMS maximising at 11 nM, ~~whereas MODIS-DMS is 64% greater, maximizing~~ while when a variable chl-a
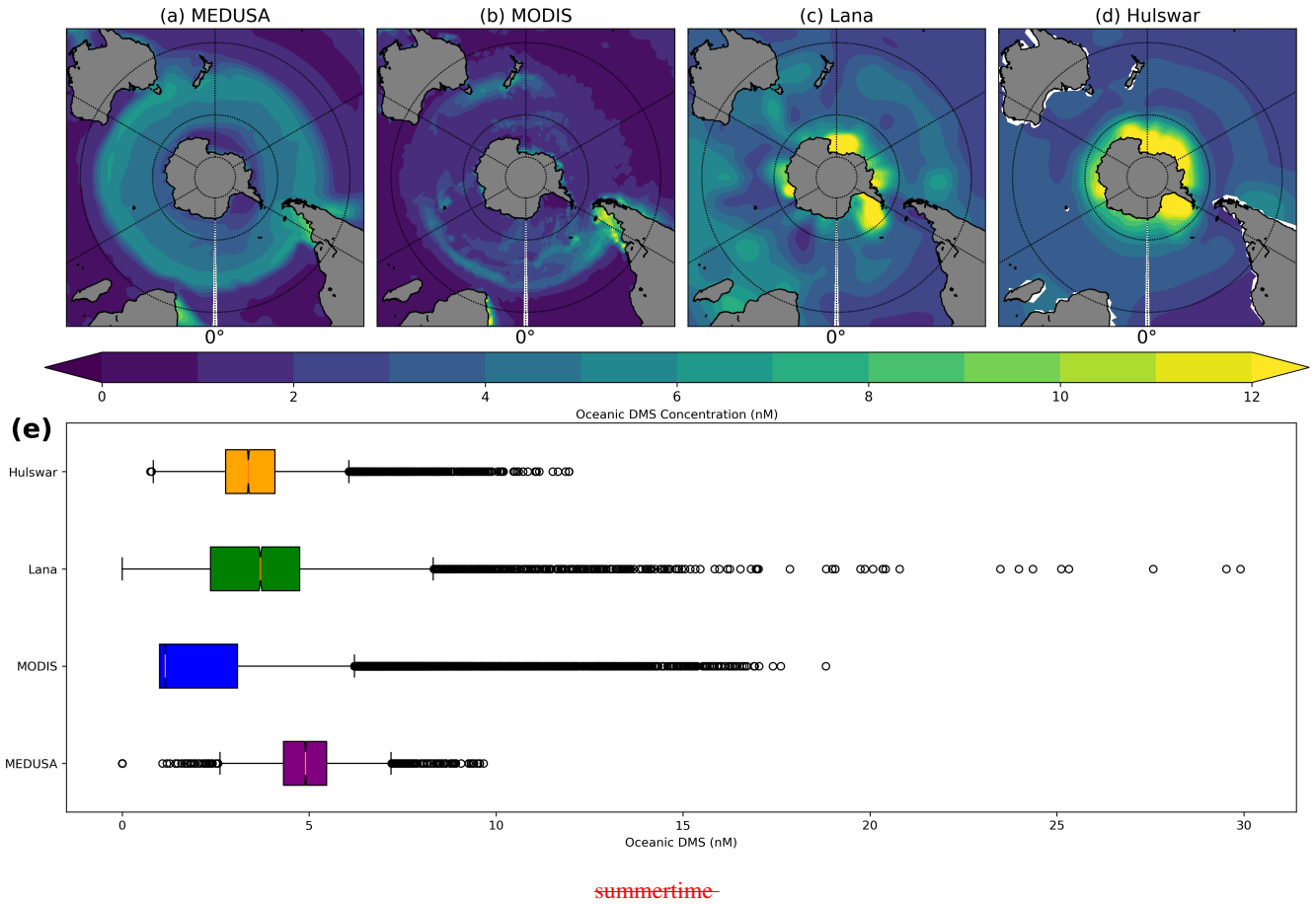
~~summertime~~

Figure 2. Summertime (DJF) Oceanic DMS in the Southern Ocean (40 - 60 °S). The spatial distribution (a-d) shows the (a) UKESM1 climatology from MEDUSA, (b) the climatology from MODIS-DMS, and observational-based climatologies of (c) Lana and (d) Hulswar. (e) The box plot shows the distribution of each oceanic DMS dataset used~~. The data points outside the whiskers represent 0.7%~~, where MODIS-DMS contains all 10 years of ~~the dataset~~data, ~~highlighting~~ while the ~~outliers of the distribution~~climatologies contain 12 months.

concentration field is used in the MODIS-DMS simulation, oceanic DMS maximises at 18 nM (64% higher than in the MEDUSA simulation).

~~By examining localized oceanic DMS measurements within the Southern Ocean obtained during the~~ To examine how the simulations compare with observations, we compare the oceanic DMS distribution against TAN1802 and SOAP voyages for the regions and times at which those voyages took place (Figure 3~~) and SOAP (~~, Figure 4)~~voyages in comparison to each model input data, we can determine the variations across each simulation. The oceanic DMS from the model overlays the respective voyage data (grey)in Figure 3 and Figure 4. Lana fits~~. For the TAN1802 voyage (40–70°S, 180°E), the distribution of ~~TAN1802 more closely than the other datasets, as illustrated by the higher DMS concentrations. The differences between the two climatologies are a result of additional observational datasets within Hulswar.~~ measured oceanic DMS aligns closely with the Lana simulation. MODIS-DMS and MEDUSA have ~~the lowest means ,~~ lower means of 1.19 and 1.52 nM, respectively, but MODIS-DMS has a ~~higher~~ high CoV of 79% due to higher concentrations at lower latitudes (45 °S) of the Southern Ocean. ~~TAN1802 has a CoV of 105%, similar to Lana's 114%. Hulswar~~ Oceanic DMS in the Hulswar simulation overestimates DMS concentrations by a factor of two between ~~45 and 65~~45–65 °S. ~~Observation-based climatologies capture high oceanic DMS concentrations better than parameterization-based concentrations, as illustrated by the violin plot in Figure 3.~~

~~SOAP voyage data represents oceanic DMS concentrations during~~ For the SOAP voyage, which targeted phytoplankton bloom events ~~, therefore the shape of the observed DMS distribution (Fig. 4) is quite different to~~ (42–47°S, 172–180°E), the measured DMS distribution is skewed toward higher concentrations compared with the TAN1802 ~~data (Fig. 3)and would be expected to be highly biased. All of the oceanic DMS datasets~~ voyage (Figure 4). In contrast, TAN1802 transected the Southern Ocean without specific focus on bloom activity, yielding a range of DMS concentrations. We consider that SOAP is still useful as it offers insights into extreme conditions not reflected in other data sets. All simulations fail to capture the higher concentrations measured by SOAP~~, displaying a positively skewed distribution (Bell et al., 2015); with most concentrations clustered between 2-4 nM.~~. Oceanic DMS in the MODIS-DMS ~~has the greatest~~ exhibits the highest variability (CoV of 36%), ~~highest average, and largest~~ mean, and maximum concentration. MODIS-DMS also ~~has the best linear relationship~~ aligns best with SOAP, ~~where~~ in that it captures some of the high DMS concentrations resulting from phytoplankton blooms. The MODIS-DMS ~~follows the concentrations through space and time better than the other datasets. For example, when SOAP measures its lowest oceanic DMS concentrations following the voyage,~~ simulation captures around half of the variability of SOAP measurements, whereas the other simulations only match between 7% to 18%. MODIS-DMS ~~also simulates its lowest concentrations. Additionally, when SOAP observations are at their highest concentrations (25 nM), MODIS-DMS displays its highest concentration (over 10 nM)~~is within 11% of the SOAP mean, whereas the other simulations are 22% to 218% lower. See Figure ?? and ?? for simulated comparisons of DMS emission to SOAP and TAN1802.

~~Lana, Hulswar, and MEDUSA fail to represent high biological variability in the Chatham Rise region of the Southern Ocean, as confirmed via comparison with TAN1802 between 45 °S to 60 °S. MODIS-DMS does not capture the heightened concentrations from SOAP or TAN1802, but it aligns more closely with the observations than the climatologies. This is likely due to the MODIS-DMS simulations using the chl-*a* data during the period of each voyage, and nudging model conditions to~~
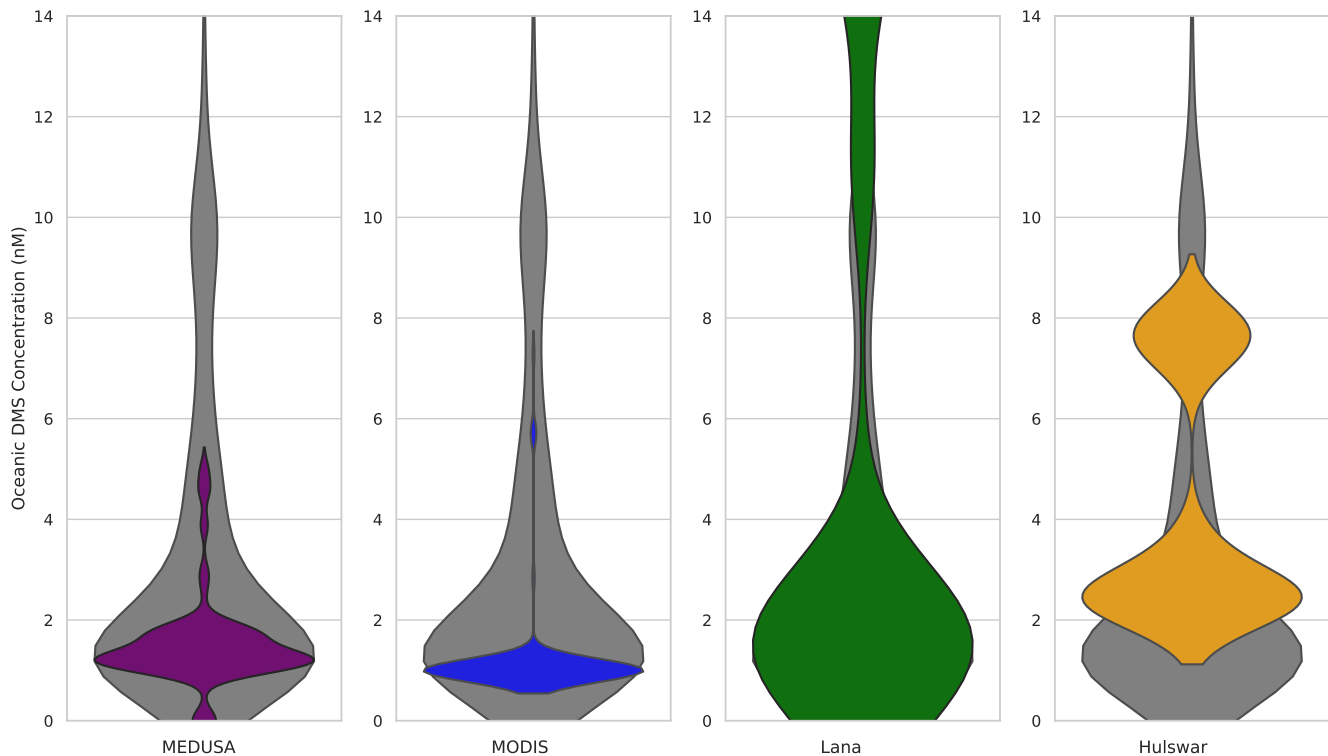
Figure 3. Violin plots of TAN1802 data (grey). Overlaid are the oceanic DMS datasets used in the model simulations (Feb to March 2018, 40 °S to 70 °S, 180 °E) from MEDUSA (purple), MODIS-DMS (blue), Lana (green), and Hulswar (yellow). Violin plots depict data distribution and density. The width of each 'violin' corresponds to the frequency of data points within that value range, while the length indicates the range of values. The frequency axis, represented by the width, allows for an immediate visual comparison of how often particular ranges of values occur in each category. This offers a comprehensive view of both the distribution and frequency of data across different categories.

similar conditions. From this, implementing the inclusion of satellite chl-*a* in oceanic DMS calculations improves the accuracy
365 of DMS distribution in lower latitudes.

The Anderson et al. (2001) oceanic DMS parameterization assumes chl-*a* has a central role in forming oceanic DMS . The known global correlation is central to oceanic DMS formation. Previous correlations between chl-*a* and oceanic DMS, described given by the coefficient of determination (rR^2), is between range globally from 0.11 to 0.818, where higher latitudes tend to have higher r0.93, with higher latitudes having increased R^2 values due to factors like nutrient availability and prolonged
370 summer daylight, coupled with heightened wind speeds (Uhlig et al., 2019; Townsend and Keller, 1996; Tison et al., 2010; Matrai et al., 1993). The Anderson et al. (2001) parameterization used Gros et al. (2023) estimated an R^2 of 0.93 towards sea ice latitudes, while Bell et al. (2021) found chl-*a* explains just 15% of oceanic DMS variability. Using the Anderson et al. (2001) parameterization in MODIS-DMS, has a strong rwe determined a large R^2 value of 0.75 in the Southern Ocean, validating
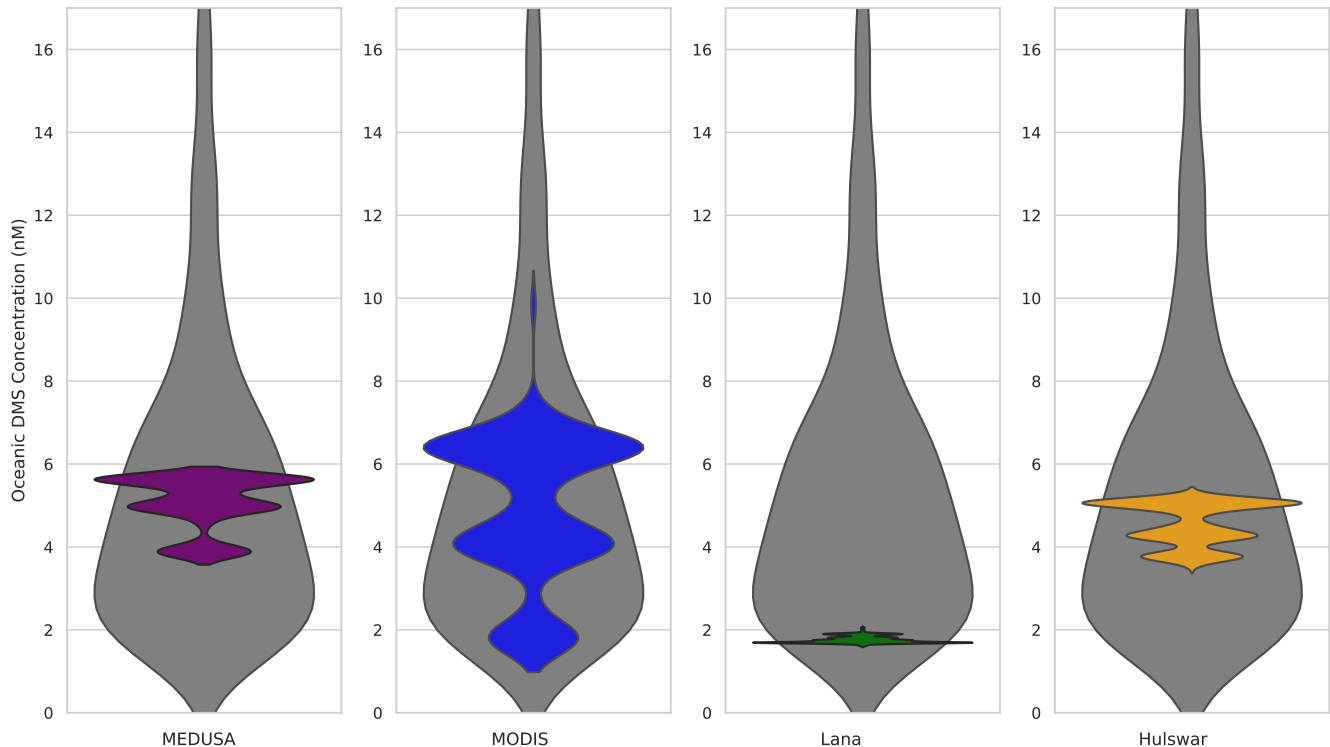
Figure 4. Same as Figure 3, but for the SOAP 2012 voyage (Feb to March 2012, 42–47 °S, 172–180 °E).

this parameterization for simulating oceanic DMS . The Anderson et al. (2001) parameterization using . While associating chl-a with oceanic DMS has discrepancies (Gros et al., 2023; Bell et al., 2021), we show that using Anderson et al. (2001) with satellite chl-a provides a better representation of austral summer oceanic DMS conditions within the Southern Ocean data better represents Southern Ocean summertime DMS compared with the Anderson et al. (2001) MEDUSA configuration.

Chl-a is used to calculate oceanic DMS within half the Earth System Models in two of the four ESMs with interactive biogeochemistry participating in CMIP6 (Bock et al., 2021). These models reveal discrepancies between each other and observed oceanic DMS data sets, indicating ongoing uncertainties in CMIP6 ESMs concerning oceanic DMS and its flux to the atmosphere (Bock et al., 2021). Bock et al. (2021) emphasizes the need for enhanced understanding and observations to accurately capture DMS–climate feedbacks. CNRM-ESM2-1 uses a comprehensive prognostic approach that considers grazing by adopts an approach considering zooplankton and DMSP , rather than chl-a. However, this is very difficult to validate due to the lack of widespread data availability. Here we suggest that a realistic biological proxy, such as chl-a, is useful to construct an oceanic DMS dataset, but its validation is challenging due to limited observational data (Belviso et al., 2012). NorESM2 uses an alternative mechanism for DMS production, by using detritus export production and sea surface temperature (Tjiputra et al., 2020). An oceanic DMS algorithm developed by Galí et al. (2018) includes sea-surface temperature, chl-a, photosynthetically active radiation, and the mixed layer depth, where but oceanic DMS has a general overestimation along

coastal regions (Galí et al., 2019; Hayashida et al., 2020). Galí et al. (2018) also produced a time series of oceanic DMS
over parts of the Northern Hemisphere, finding ~~similar~~ high inter-annual variability ~~by~~ using chl-a satellite data. ~~We concur with Galí et al. (2018) that a move beyond classical climatologies is an important step in developing future climate models. We suggest using temporally varying input instead of climatology to allow the capture~~ Adopting temporally variable oceanic DMS inputs within the model may better reflect inter-annual ~~variability over the Southern Ocean , particularly from~~ Southern Ocean variability due to ENSO events and biologically productive years. One such way to achieve this for future projections would be through a stochastic approach of capturing all chl-a years from the satellite (e.g. SeaWiFS and MODIS-aqua) archive~~, including high biological productivity years, such as 2010 and 2020, or low productivity such as in 2015 (Figure ??)~~.

3.2 DMS Flux

Having established that ~~the~~ oceanic DMS from the MODIS-DMS ~~data set produces simulated oceanic DMS in good agreement with observations (~~simulation aligns well with summertime observational voyages as seen in Figure 3~~),we now test~~, 4, we now assess the sensitivity of atmospheric DMS to ~~a suite of~~ various sea-to-air transfer functions ~~for different oceanic DMS sources~~(Figure 5, ??). Figure 5 shows the DMS flux during ~~austral summer across all simulations integrated over~~ the austral summer in the Southern Ocean~~region (40 to 60 °S), which ranges, on average,~~ , averaging between 2.9 to 7.3 TgS Yr^{-1}. ~~The spread of~~ This is consistent with Jarníková and Tortell (2016) estimation of 3.4 Tg S, aligning most with the MODIS-DMS linear parameterizations (LM86 and B17). The spread in average Southern Ocean summertime DMS fluxes across the ~~mean fluxes across all~~ eight simulations is 153%, which is greater than the ~~difference~~ spread between all the ~~oceanic DMS inputs, a~~ simulations testing different oceanic DMS sources, at 107%~~spread in mean oceanic DMS concentration~~. The lowest ~~CoV value~~ CoVs within both oceanic DMS and DMS emissions are found in the MODIS-DMS simulations, specifically, the Blomquist et al. (2017) parameterization (MODIS$_{B17}$) with a mean of 2.9 ± 0.84 TgS Yr^{-1}. The upper range of simulated DMS flux, 7.3 ± 1.8 TgS Yr^{-1}, comes from the W14 quadratic formula used with the Lana DMS climatology (Lana$_{W14}$).

The largest DMS emissions are seen in the MEDUSA$_{LM86}$ simulations, due to the relatively large underlying seawater DMS source spread throughout the Southern Ocean (Figure 2a). The Lana$_{w14}$ simulation also shows large DMS emissions due to the quadratic dependence of the gas transfer velocity on wind speed (Figure 1). Overall, the W14 quadratic formula yields about 33% more emissions than the LM86 ~~has a~~ and B17 linear formulas. For the transfer velocity parameterizations using a linear relationship to wind (LM86 and B17), LM86 exhibits a higher transfer velocity than B17 for wind speeds ~~greater than~~ above 7.5 m s^{-1} (Figure 1). ~~The Southern Oceanhas the highest wind speeds over any ocean region, with wind speeds very frequently above 7.5 m s^{-1} (Bracegirdle et al., 2020b), therefore our simulations show Liss and Merlivat (1986) flux produces~~ Given the Southern Ocean's predominant high wind speeds (Bracegirdle et al., 2020a), simulations indicate that LM86 yields 14% more ~~emissions of DMS than Blomquist et al. (2017)~~ emitted DMS than B17 (Figure ~~1)~~. ~~Lana is widely used by climate models (e.g. Sellar et al., 2019; Horowitz et al., 2020; Bhatti et al., 2022). Implementing a DMS flux based on DMS observations within this climatology (Lana$_{B17}$) results in a 4.86 ± 1.67 TgS Yr^{-1} flux, which is within the range of all the simulations (Figure~~ 5).
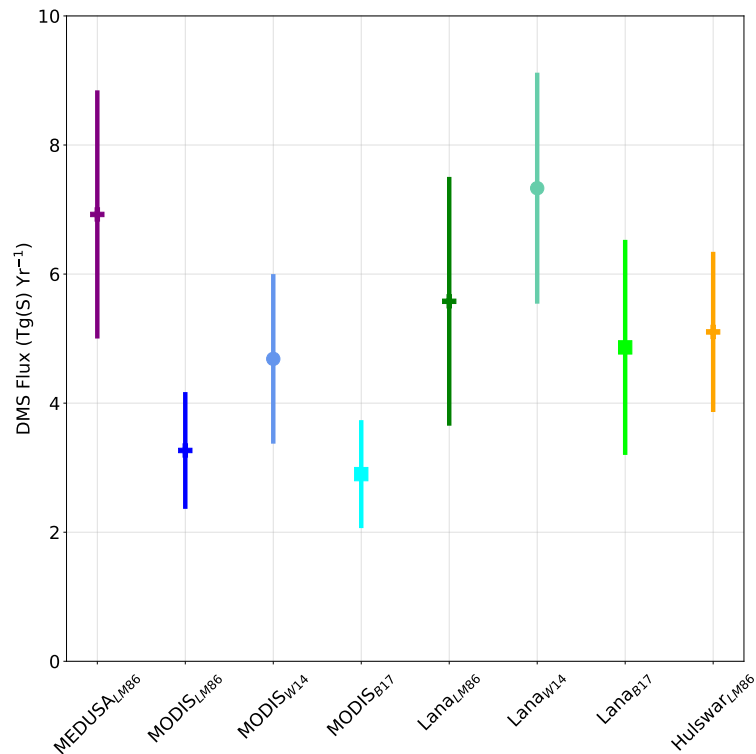
Figure 5. Summertime (December – February) Southern Ocean sulfur emissions in Tg Year^{-1} in all model simulations performed. The error bars represent the spatial and temporal standard deviation. The different colors represent different oceanic DMS climatologies (Purple: MEDUSA ((Sellar et al., 2019; Anderson et al., 2001), Green: (Lana et al., 2011) and Orange: Hulswar ((Hulswar et al., 2022), and time series (Blue: derived from MODIS-DMS chl-a) used in this work. + marker represents simulations performed with the Liss and Merlivat (1986) sea-to-air flux, the dot marker represents Wanninkhof (2014), and the square marker represents Blomquist et al. (2017).

~~For simulations using the same~~ The LM86 ~~sea-to-air flux parameterizations, but different~~ flux parameterisation was tested with all oceanic DMS sources, ~~the spread of all means is~~ as it is currently the parameterisation used by default in UKESM1-AMIP. Simulations using LM86 have a spread in average summertime Southern Ocean DMS emissions of 112% (3.3 to 6.9 TgS Yr^{-1}).

425 ~~The means derived from different DMS~~ In contrast, simulations using the same oceanic DMS source (MODIS-DMS and Lana) ~~but~~ flux parameterizations (LM86, B17, and W14) ~~within MODIS-DMS and Lana are spread between~~ have a spread in average summertime Southern Ocean DMS emissions of 51% (MODIS-DMS simulations) to 62% (Lana simulations). The choice of the oceanic DMS source ~~is therefore more important than the choice of DMS emission flux. Changing oceanic DMS within the model produces a larger impact on the resultant atmospheric DMS than the flux parameterization used. The emission of DMS~~

430 ~~from the ocean, over the Southern Ocean, results in a slightly higher spread between all the simulations of 6%. For a given oceanic DMS source, the quadratic formula of W14 produces around 33% more DMS emissions than the linear formulas of LM86 and B17~~ therefore impacts DMS emissions more than the transfer velocity parameterization within these simulations.

~~The selection of a DMS flux parameterization has a large impact on the emissions of oceanic DMS. The W14 parameterization~~
~~generates excessive DMS emissions, accurately representing the highest 10% (see Figure ??) but overestimating the rest of~~
~~the distribution. Using W14, or similar quadratic fluxes (such as Nightingale et al. (2000)) within climate models for DMS~~
~~emissions could therefore result in an overproduction of DMS. See Figure ?? for a visual overview of DMS across all~~
~~simulations.~~

Table 3 ~~presents simulated daily Southern Ocean DMS fluxes~~ details simulated daily DMS fluxes over the Western Antarctic Peninsula during the austral summer. ~~The total annual DMS emissions which occur during DJF are presented as a percentage~~ ~~and as a daily flux. DMS emissions during austral summer make up 32-46~~, for comparison with observations, including Webb et al. (2019). DMS emissions in this period constitute 33-52% of the annual flux, ~~substantially lower than~~ contrasting with the 72% reported by Webb et al. (2019). ~~However, Webb et al. (2019) measured DMS in Ryder Bay, near the Antarctic Peninsula (67.54 °S, 68.35 °W), an area known for high levels of~~ The region exhibits significant sea-ice melt and high DMS emissions during DJF. ~~The~~ Our simulations daily mean flux ~~from our simulations~~ during DJF is $\overset{\sim}{22.2}$ 4.6 $\pm$ ~~5.13~~ 4 μmol m^{-2} d^{-1}. ~~Compared with the 22.7~~, below Webb et al. (2019)'s 29 μmol m^{-2} d^{-1} ~~flux reported by Webb et al. (2019)~~ for Ryder Bay ~~during the summer, our simulations therefore represent fluxes within the expected range. Additionally, a~~ (67.54 °S, 68.35 °W). However, our results align with the emissions from Jarníková and Tortell (2016); Berresheim et al. (1998); Asher et al. (2017). Like in Jarníková and Tortell (2016) and Webb et al. (2019), we find periodic hot spots of DMS emissions above 50 μmol m^{-2} d^{-1} over these sub-Antarctic regions, but at 10% the magnitude of the maximum found by Webb et al. (2019).

A 2018 Southern Ocean voyage during February ~~calculated~~ reported a mean daily flux ~~to be between~~ of 2.6 $\pm$ 3.5 μmol m^{-2} d^{-1} ~~within~~ over the open ocean (Zhang et al., 2020). ~~Tracking this voyage through space and time with our simulations shows fluxes varied between~~ Our simulations are in good agreement with this, showing DMS fluxes of 2.7 μmol m^{-2} d^{-1} ~~from~~ (MODIS$_{B17}$) to 8.9 μmol m^{-2} d^{-1} ~~in~~ (Lana$_{W14}$) for the same region and period of time. Shon et al. (2001) estimated ~~the daily flux between 40 °S to 55 °S around early December to be~~ a daily flux of 2.6 $\pm$ 1.8 μmol m^{-2} d^{-1} ~~.~~ ~~Only~~ around early December. Only the MODIS$_{B17}$ ~~coincides with~~ simulation matches these daily fluxes ~~across this latitudinal region. Our~~. Furthermore, the linear MODIS-DMS simulations ~~using a linear flux parameterisation (LM86 and B17) also align~~ (MODIS$_{LM86}$ and MODIS$_{B17}$) are in good agreement with the 12 $\pm$ 15 μmol m^{-2} d^{-1} measured by Marandino et al. (2009) and the 2.8 μmol m^{-2} d^{-1} measured by Lee et al. (2010) in the Southern Ocean.

~~Pandis et al. (1994) estimates that for aerosol nucleation to occur from DMS emissions, the flux must be above 2.5 μmol m^{-2} d^{-1}. Our simulations show that DMS emissions are above this threshold between 52% (MODIS$_{B17}$) and 88% of the time (MEDUSA$_{LM86}$) during summertime. This range agrees with Webb et al. (2019), who measured the flux to be over this threshold around 63% of the year. MODIS$_{LM86}$ (at 61%) and Lana$_{LM86}$ (at 62%) compare best to the observed value, although Webb et al. (2019) is likely positively skewed based on their location in an area characterised by large DMS emissions. As the UKESM1 underestimates AOD during austral summer (Mulcahy et al., 2020), MEDUSA$_{LM86}$ also produces the highest daily DMS flux over the Southern Ocean, suggesting a bias may be present during the formation of aerosols. This may be a result of the chemistry scheme used in the formation of aerosols as a compensating bias, which will be addressed in future work.~~

Table 3. Mean daily DMS flux over the ~~Southern Ocean~~ Western Antarctic Peninsula, by Ryder Bay during the austral summer period for each simulation. The percentage shows the proportions of the total annual DMS flux which occurs during the summer months. Additionally, the total DJF flux shows the mean daily DMS flux (μmol m^{-2} d^{-1}) and standard deviations. ~~The last row outlines the overall DMS flux volume, simulated above the 2.5 μmol m^{-2} d^{-1} threshold for aerosol nucleation to occur from DMS emissions, as a percentage.~~

	MEDUSA$_{LM86}$	MODIS$_{LM86}$	MODIS$_{W14}$	MODIS$_{B17}$	Lana$_{LM86}$	Lana$_{W14}$	Lana$_{B17}$	Hulswar$_{LM86}$	Webb et al. (2019)
Total DJF %	~~38.1~~ 44	~~31.8~~ 34	~~31.7~~ 33	~~44.9~~ 36	~~40~~ 49	46	~~40.3~~ 52	46	72
Total DJF (μmol m^{-2} d^{-1})	~~31.8~~ 4.3 ± ~~5.9~~ 4	~~15.3~~ 2.2 ± ~~2.7~~ 2.5	~~21.6~~ 2.7 ± ~~3.8~~ 3	~~13.3~~ 1.9 ± ~~2.6~~ 2	~~26.1~~ 5.6 ± ~~4.6~~ 5.1	~~34.4~~ 8.4 ± ~~5.5~~ 7.5	~~22.3~~ 5.3 ± ~~3.9~~ 4.2	24 6 ± 3.7 ~~Total DJF % above 2.5 μmol m^{-2} d^{-1}~~ 5.2	~~88 61 73.5 52 62 76.8 56 66~~ 29

Many CMIP6 models use the quadratic sea-to-air flux parameterization detailed in Wanninkhof (2014) ~~to calculate~~ for DMS emissions (e.g. Salzmann et al., 2022; Seland et al., 2019; Neubauer et al., 2019; Tatebe and Watanabe, 2018; Wu et al., 2019)~~, however, recent literature suggests that DMS has~~. Yet, recent studies indicate a linear relationship ~~with~~ between DMS and wind speed (e.g. Blomquist et al., 2017; Goddijn-Murphy et al., 2016; Bell et al., 2013; Zavarsky et al., 2018; Vlahos and Monahan, 2009; Bell et al., 2015). We ~~show~~ demonstrate that linear DMS ~~emissions may not represent the upper ranges of DMS flux as well as quadratic flux emissions, where wind and oceanic DMS concentrations are high. Extreme concentrations of oceanic DMS can result in very high emissions. Lana$_{W14}$ simulates these higher concentrations similar to the higher fluxes from TAN1802 (Figure ??) but result in an overestimation for the lower emissions of the distribution. MEDUSA$_{LM86}$ emits DMS similarly to the quadratic formulation of Lana$_{W14}$, within the higher ranges of emissions. Therefore, using a formula developed specifically for DMS, such as Blomquist et al. (2017) may generally better represent DMS emissions in the UKESM1. Additionally, simulations of atmospheric DMS with UKESM1 are improved when using observed chl-a concentrations to calculate historical oceanic DMS~~transfer velocities represent the DMS flux ranges better than the quadratic W14 flux when compared to Southern Ocean observations.

3.3 Atmospheric DMS

~~We now~~ We next evaluate atmospheric DMS in our sensitivity simulations. Figure 6 compares all simulated atmospheric DMS ~~concentrations to observational data averaged across the Southern Ocean during austral summer. The observational data shown~~ with observational datasets. Data in Figure 6 ~~was collated from three observational stations (Cape Grim, Amsterdam Island, and King Sejong Station) and three~~ is from three Southern Ocean voyages (SOAP, SOIREE, ~~and ANDREXII), with an average and a standard deviation (spatial and temporal)~~summertime atmospheric DMS concentration of 185 ±~~ ANDREXII; Figure 6a-c) and two stations (Cape Grim and King Sejong Station; Figure 6d-e). Figure 6f shows aggregate averaged DMS concentrations from all five observational sources, and has an average summertime concentration of 129 ~~ppt (Smith et al., 2018; Wohl et al., 2020; Boyd and Law~~. The mean atmospheric DMS across all simulations is 276 ± 174 ppt, and is within the range of the observations. In addition, when using the DMS source in best agreement with oceanic observations (~~74 ppt (Smith et al., 2018; Wohl et al., 2020; Boyd and Law, 200~~. The simulations using the MODIS-DMS ~~) combined with a linear DMS flux parameterisation~~ oceanic source and linear DMS transfer models (LM86 and B17) ~~, the atmospheric concentration mean is consistent~~ show the closest agreement with the observational mean, ~~averaging 164~~ of 106 ± 132 ppt ~~. Along the Peruvian coastline, Zhao et al. (2022) measured atmospheric~~

~~DMS concentrations at 145~~ 66 ppt and 100 ± ~~95 ppt, which also aligns well with the linear MODIS-DMS simulations. During the summer months,~~ 60 ppt for MODIS$_{LM86}$ and MODIS$_{B17}$, respectively. The mean total spread in summertime Southern Ocean atmospheric DMS across all simulations is 171%, compared with the spread of 153% in DMS emissions.

Our simulations, compared to coastal Antarctic measurements, offer insights into the performance of sea ice-influenced regions (Galí et al., 2021). In summer, Berresheim et al. (1998) recorded mean atmospheric DMS ~~concentrations~~ of 119 ppt ~~(measured~~ at 64.8 °S, 64 °W~~) by Berresheim et al. (1998) and 114 ppt(measured~~, closely matching MODIS$_{B17}$ at 121 ppt. All other DMS sources show concentrations which are more than twice as large as this measurement. Read et al. (2008) measured atmospheric DMS concentrations of 45 ± 50 ppt at Halley Station, Antarctica (75.4 °S, 26.2 °W)~~by Read et al. (2008) align best with the MODIS-DMS simulations . Additionally, Lee et al. (2010) measured a mean of 61 ppt over the same high latitudes in February. However, there are also disagreements between observations and MODIS-DMS simulations with linear fluxes, as a voyage tracking along the Eastern South Pacific Ocean during January 2000 measured 340~~, best aligning with Lana$_{B17}$ at 42 ppt. It should be noted that all simulations fall within one standard deviation of the measurements reported at Halley Station.

Preunkert et al. (2007) measured high interannual variation of atmospheric DMS at Dumont d'Urville (66.4 °S, 140 °E) during January, from 244 ppt in 2002 to only 60 ppt in 2003. The average January concentration over 13 years was 170 ± ~~370 ppt (Marandino et al., 2009), which is consistent with Lana~~180 ppt. Here, the Lana and Hulswar simulations are in closest agreement, and simulate average DMS concentrations between 92 and 141 ppt. Lastly, Lee et al. (2010) measured a 61 ppt average over the Pacific Southern Ocean in February, closest to MODIS$_{B17}$ and MODIS$_{LM86}$ ~~, but not as high as Lana$_{W14}$.~~ ~~The variability from Amsterdam Island measurements is much higher than that of the simulations.~~ (64 and 53 ppt, respectively).

~~These measurements highlight the high variability of atmospheric DMS~~ Multi-annual studies emphasize high yearly variability (Read et al., 2008; Preunkert et al., 2007). Measurements during austral summer over the Southern Ocean show significant variability, especially in higher latitudes. The climatologies produce higher concentrations along the coastal regions of Antarctica, as illustrated in Figure 2a-d, but MODIS-DMS still captures much of the spatial variability (Figure ??). MEDUSA performs the worst over these higher latitude regions, where sea ice can have a large role in producing atmospheric DMS (Galí et al., 2021). ~~Berresheim (1987) measured 106 ppt over the Drake passage during March and April, representing the lower end of our simulated DMS mixing ratio. All measurements during summer show very high variability , with lower values seen in higher latitudes.~~ MODIS$_{B17}$ ~~does a better job of representing atmospheric DMS compared to simulations from other~~ represents atmospheric DMS more accurately than models like MEDUSA, Lana, and Hulswar ~~when compared to observations~~ based on observations over the Southern Ocean during summertime.
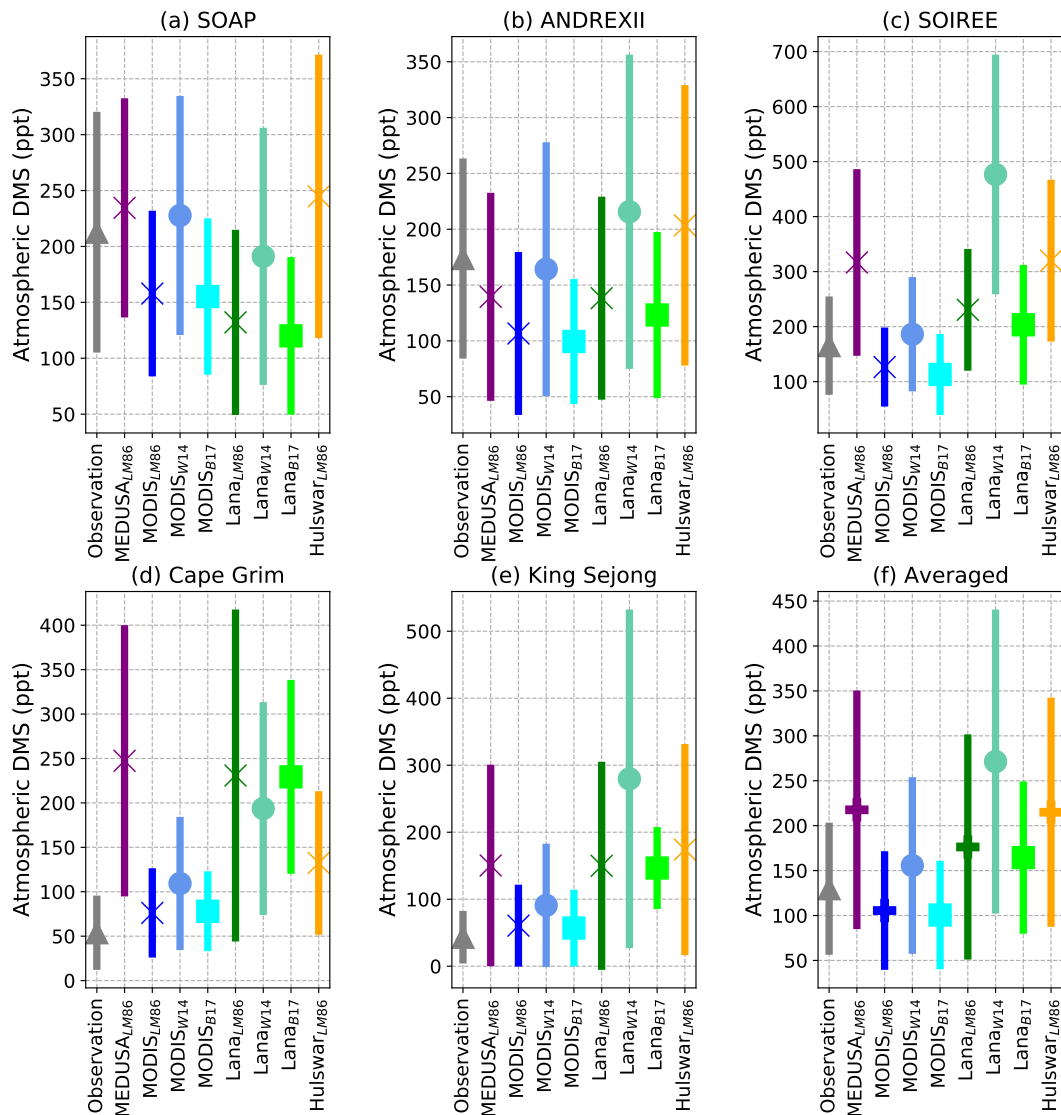
Figure 6. Five observational datasets measuring atmospheric DMS concentrations (ppt) are directly compared with the eight simulations (a – e) at the same spatial and temporal resolution. In (a) SOAP and (b) ANDREXII, we follow both voyages using the nearest grid cell along each hour of the simulations, matching the timescales in 2012 and 2019. For comparing the simulations with the (c) SOIREE voyage, we also follow this voyage in an hourly timescale, but due to the voyage being outside our study period, we average this over all 10 years. The two observational stations used are (d) Cape Grim and (e) King Sejong Station. We calculate the nearest grid-cell for each simulation to the observational station and constructed an average over 10 years along with a temporal standard deviation. From this, we construct an overall average (f) and standard deviation for all observational measurements and simulations which can be compared directly to these observations.

3.4   Effects from Inter-annual and Spatial Variability
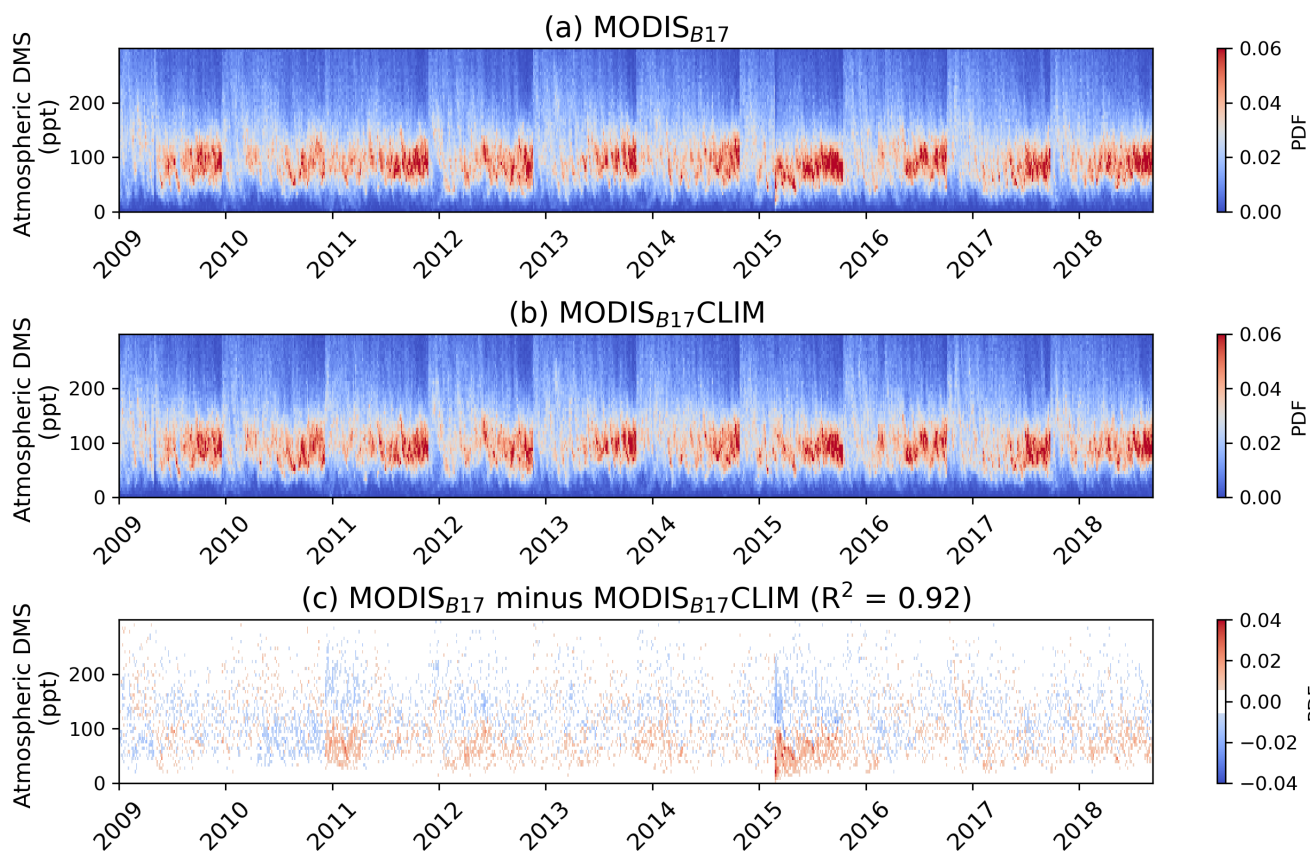
~~DJF averaged~~

Figure 7. ~~Time series of the~~ atmospheric ~~concentration~~ DMS probability density function between ~~(ppt) for the nine simulations. The~~ ~~observations represent a~~summertime average across ~~Cape Grim, Amsterdam Island,~~) MODIS$_{B17}$ and ~~King Sejong Station and three~~ (b) MODIS$_{B17}$CLIM from 2009 to 2018 summer over the entire Southern Ocean~~voyages~~. ~~(SOAP, SOIREE, and ANDREXIIc)~~. ~~The error bars~~ ~~represent~~ the ~~standard deviation through time~~ difference between MODIS$_{B17}$ and ~~space~~MODIS$_{B17}$CLIM is also shown, with the R^2 shown between the two simulations.

~~So far we have focused on DMS, which is an important biogenic marine aerosol precursor. However, the development of~~ To assess the impact of interannual variability in oceanic DMS on simulated atmospheric DMS, we compare the MODIS$_{B17}$ simulation with MODIS$_{B17}$CLIM, which used a climatology of oceanic DMS calculated from the MODIS-DMS data set ~~has~~ ~~implications for primary marine organic aerosol (PMOA), whose production is influenced by~~ (Figure 7). Both simulations are similar (R^2 = 0.92) in terms of interannual variability across the Southern Ocean as a whole. (Figure 7c). Rolling means are presented in Figure **??**b, c. While there are small differences in Southern Ocean atmospheric DMS between the simulations, the overwhelming similarities between Figure 7a and b suggest that an oceanic DMS climatology results in similar interannual

530 variability in the atmospheric DMS PDF suggesting that oceanic DMS is not a strong driver of interannual variability in atmospheric DMS. This result is in contrast to that of Galí et al. (2018) who used a different algorithm for producing oceanic DMS. This difference may be due to our use of the Anderson et al. (2001) algorithm, which is known to produce limited variability (Belviso et al., 2004; Bock et al., 2021).

To assess the impact of spatial variability in oceanic DMS on simulated atmospheric DMS, we compare simulations

535 performed using the MEDUSA and MODIS-DMS data sets (with low and high spatial variability in oceanic DMS, respectively) in Figure 8. Larger variability in the MODIS-DMS oceanic DMS source leads to larger variability in simulated atmospheric DMS, compared with the MEDUSA simulations. The spatial CoV from MEDUSA$_{LM86}$ is 45% lower than MODIS$_{LM86}$, showing greater spatial variability from MODIS-derived chl-a concentration in UKESM1 (Mulcahy et al., 2020). PMOA are organic detritus or compounds that are emitted to the atmosphere when bubbles burst as waves break (Gantt et al., 2012, 2011)

540 . A parametrisation of PMOA has been implemented in the UKESM1 in Mulcahy et al. (2020) based on the parametrisation developed by Gantt et al. (2011), where PMOA is a function of wind speed, sea salt dry diameter, and surface chl-a. As identified by Mulcahy et al. (2020), the MEDUSA chl-a bias is carried through to PMOA which results in a Southern Ocean distribution similar to that of oceanic DMS . The oceanic DMS signal in the atmosphere is strong but includes large fluctuations the wind.

545 PMOA is the dominant source of ice nucleating particles over the Southern Ocean (Vergara-Temprado et al., 2018; Zhao et al., 2021) which may reduce the downwelling shortwave radiation bias (Schuddeboom and McDonald, 2021; Fan et al., 2011; Fiddes et al., 2022) . This shortwave bias may have links to a deficit in supercooled liquid
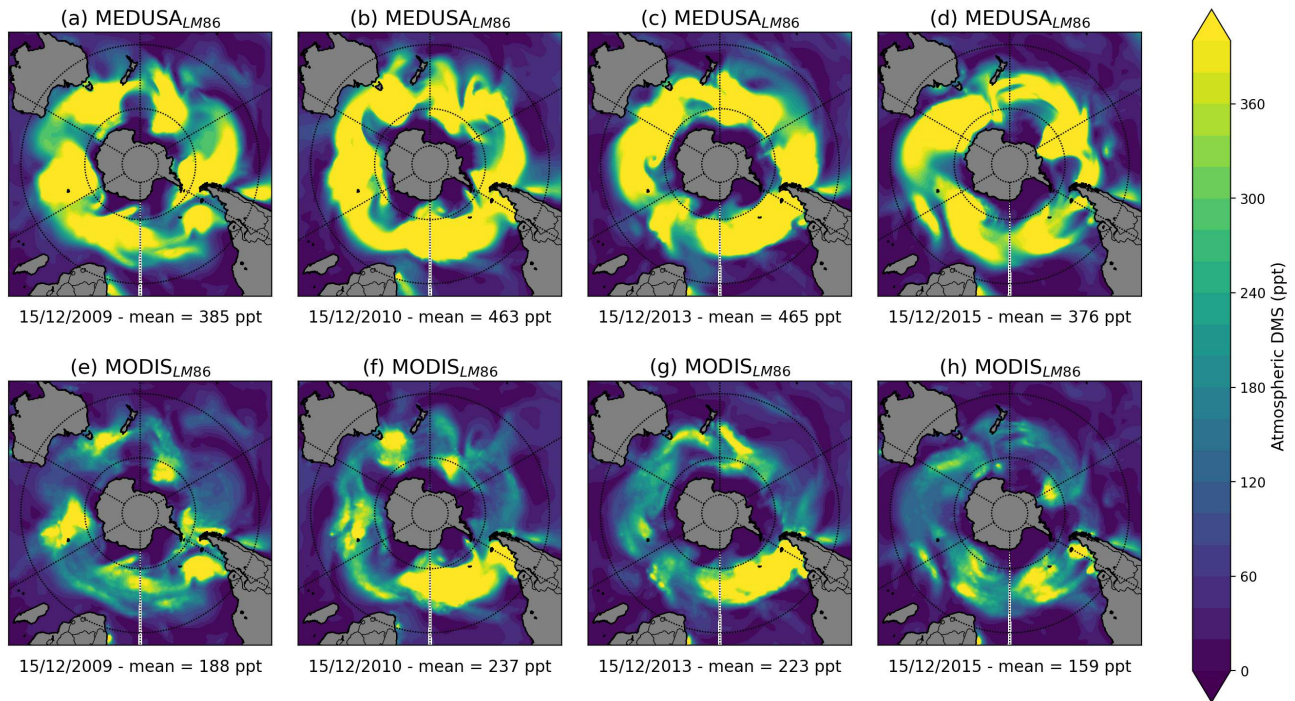
Figure 8. Atmospheric DMS concentrations comparing (a - d) MEDUSA$_{LM86}$ with (e - h) MODIS$_{LM86}$ across four of the same summertime days (15th December) in (a, e) 2009, (b, f) 2010, (c, g) 2013, (d, h) 2015. The area-weighted Southern Ocean mean is shown below each plot.

3.5   Aerosol and cloud response

Figure 9 shows the effect on cloud and aerosol properties of changing the atmospheric DMS distribution. Changing the atmospheric DMS concentration yields little change to CCN, CDNC or AOD. This suggests that these variables are significantly influenced by factors such as sea spray aerosol and the atmospheric oxidation pathways that convert DMS to sulfate aerosol (Revell et al., 2021; Fossum et al., 2020). Changes to the DMS source increase the spread in simulated CCN and CDNC over the Southern Ocean ~~within CMIP6 (Fan et al., 2011). Our analysis shows that upon implementing chl-a measurements derived into the parametrisation (Figure ??), PMOA~~ rather than changing the mean DMS emissions, which is consistent with our findings for atmospheric DMS concentrations. Altering the DMS source affects AOD by 73% more than DMS emissions over the Southern Ocean ~~increase substantially during summer (81%) . Although PMOA is in the preliminary stages of development within the UKESM1, our results increase in ice nucleating particles which could improve PMOA-driven cloud formation processes~~, emphasizing the role of the ocean in producing atmospheric DMS. Box plots of AOD, CCN, and CDNC (Figure 9e, a, c) show that the simulations do not capture the maxima in CDNC, CCN or AOD over the Southern Ocean. ~~This will be investigated in future work.~~
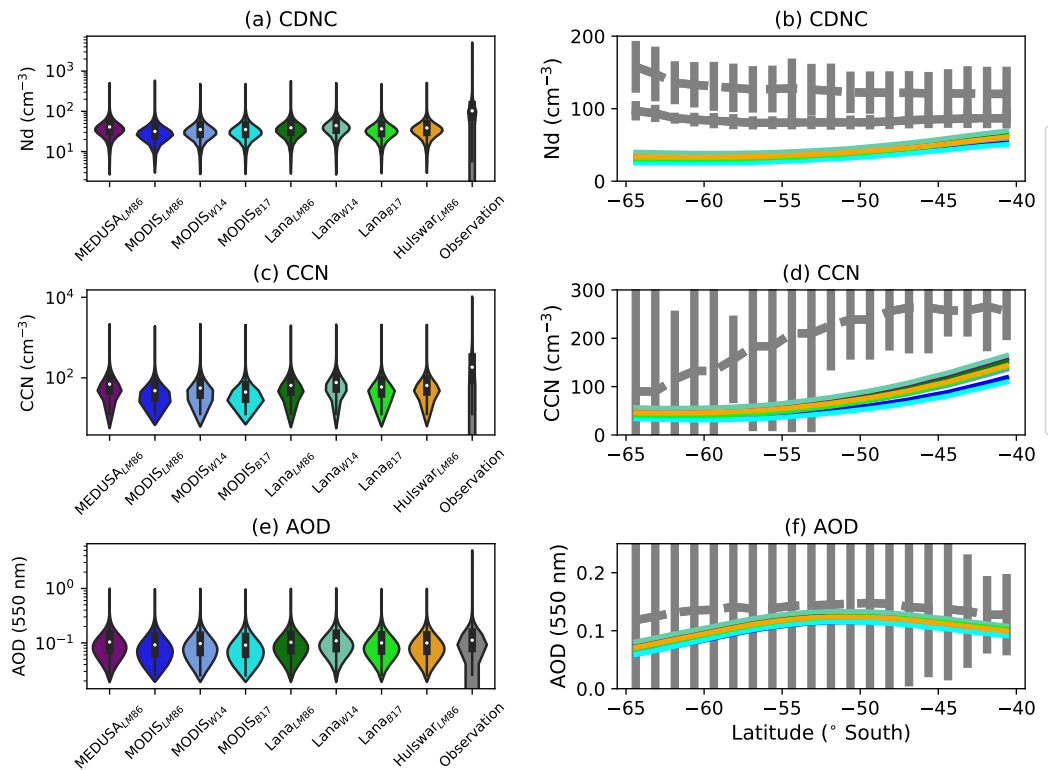
Figure 9. Summertime climatology between 60° S to 40° S showing the (a,b) cloud droplet number concentrations, (c,d) cloud conversation nuclei (800 m in altitude), and (d,e) aerosol ~~for~~ optical depth at 550 nm. The violin plots (a,c,e) ~~MEDUSA~~ represent all spatial and ~~for~~ temporal data points across the 10 years over the Southern Ocean in DJF. The lowest 1% of values are excluded from the violin plots. In (b,d,f) ~~MODIS DMS simulation integrated over~~ the ~~summer period~~ grey lines represent observational datasets where (~~DJF~~b) Grosvenor et al. (2018) (dashed) and Bennartz and Rausch (2017) (solid) are shown for CDNC, (d) Choudhury and Tesche (2023) is shown at 818m, and (f) AOD climatology by the MODIS satellite-retrieval is shown (Platnick et al., 2017). The ~~mean value is area weighted across~~ error bars represent one standard deviation either side of the ~~Southern Ocean DJF~~observational mean.

4 Conclusions

~~The concentration and distribution of atmospheric DMS is highly uncertain~~ Modelled atmospheric DMS over the Southern Ocean ~~, in part due to the lack of observational data and lack of understanding of oceanic DMS and DMS~~ is sensitive to both oceanic sources and sea-to-air emissions. We ~~examine the key processes and relationships involved in the emissions of~~ 565 ~~DMS and the production of atmospheric DMS . We also provide an overview of different oceanic DMS climatologies and~~ ~~calculate an oceanic DMS time series using chl-*a* satellite data . We then used three different oceanic DMS climatologies~~ ~~(MEDUSA, Lana, and Hulswar) in~~ examined the sensitivity of atmospheric DMS to different oceanic source data sets and sea-to-air transfer velocity parameterizations using the UKESM1-AMIP model. We also ~~constructed a competing oceanic DMS~~

demonstrate the effectiveness of using a 'MODIS-DMS' oceanic DMS data set and climatology calculated from satellite chlorophyll-a observations. MODIS-DMS

MODIS-DMS simulations indicate that large open water areas in the Southern Ocean have lower oceanic DMS concentrations compared to the other three oceanic DMS data sets tested (MEDUSA, Lana, and Hulswar). Climatologies compiled from in-situ observations (Lana and Hulswar) depict fewer distinct features in oceanic DMS concentrations than MODIS-DMS. Coastal regions have enhanced chlorophyll-a and DMS, and we demonstrate the influence of spatiotemporal chl-a fluctuations on oceanic and atmospheric DMS. Atmospheric DMS in the MODIS-DMS time series simulation shows similar interannual variability to the MODIS-DMS-CLIM simulation, indicating that capturing realistic spatial variability is more important than capturing realistic interannual variability.

Current oceanic DMS climatologies in climate models lack realistic spatial distributions for Southern Ocean summer, evident from voyage comparisons and atmospheric DMS spatial distribution. We show how using chl-a data from the MODIS-aqua satellites offers a good spatial representation of oceanic DMS. Approaches such as this and that of Gali et al offer promising avenues for realistically capturing spatial variability in oceanic DMS associated with marine biogenic activity. The current approach to calculating oceanic DMS within UKESM1 (MEDUSA) shows little spatial variability and high average biases in the Southern Ocean region, emphasizing the need for further refinement (e.g. Bock et al., 2021; Mulcahy et al., 2020; Yool et al., 2021).

We find that atmospheric DMS sensitivity to oceanic DMS changes surpasses the sensitivity to flux parameterizations in our study. Different oceanic DMS concentrations, using the same sea-to-air parameterization, lead to a 112% spread across the means within the DMS emissions. In contrast, changing just the DMS flux parameterization alone results in a 50-60% spread. The total spread in average Southern Ocean DMS emissions across all simulations is 153%, while the atmospheric DMS concentration spread is 171%. Both oceanic DMS and DMS flux parameterization concentrations and emissions, thus requiring careful

~~thought about implementation in future simulations~~changes significantly influence atmospheric DMS, emphasizing the need for careful consideration in future research.

~~We recommend moving away from the commonly used W14 quadratic sea-to-air flux parameterization in CMIP6 models for DMS and instead consider more up-to-date relationships developed specifically for DMS.~~ The Wanninkhof (2014) quadratic DMS parameterization ~~has a~~ leads to 33% ~~larger influence on~~ more DMS emissions than ~~that of~~ Liss and Merlivat (1986) and Blomquist et al. (2017). ~~Additionally, all simulations have a summertime Southern Ocean flux of 22.2 ± 5 μmol m^{-2} d^{-1}, with linear flux parameterizations aligning~~ Linear transfer velocity parameterizations align better with observations ~~than the quadratic flux. Furthermore, we found that using~~ for DMS emissions, particularly for the MODIS-DMS simulations. Using a linear flux parameterization ~~, B17, and LM86,~~ within MODIS-DMS ~~aligned the~~ brought atmospheric DMS (~~164~~88 $\pm$ ~~132~~ ppt) ~~much closer to the observations (185~~55 ppt) closer to observations ($108 \pm$ ~~129~~61 ppt). ~~All simulations have a Southern Ocean DJF mean of 276 ± 174 ppt, within one standard deviation.~~

~~The use of climatologies within climate models to represent oceanic DMS does not represent realistic distributions within the Southern Ocean as shown by comparisons to voyages. Climatologies should be replaced by spatially distributed time series to represent inter-annual variability of oceanic DMS. The time series would benefit from using a wide-spread readily available dataset that best represents a realistic spatial distribution of oceanic DMS. Given the current data availability, using chl-*a* data from the MODIS-aqua satellite is a viable option. The oceanic DMS within the UKESM1 (MEDUSA) is positively biased (e.g. Bock et al., 2021; Mulcahy et al., 2020; Yool et al., 2021), and is in need of further development. In futurework, when developing sulfate chemistry, we recommend using the LM86 or~~ In future, we recommend that models use up-to-date DMS-specific relationships such as B17~~flux parameterization along with either Lana or MODIS-DMS oceanic DMS concentrations, to capture a more realistic DMS cycle in the Southern Ocean.~~

Author contributions. Author contributions. YAB implemented model developments, performed model simulations and wrote the manuscript with assistance from all co-authors. LER, AJM and AJS assisted with the experimental design and the model evaluation compared with the observational datasets and sensitivity analysis. ATA advised on DMS chemistry and aerosols over the Southern Ocean. CH provided assistance for lodging DMS emissions into the UKESM1 trunk. JW and EB provided technical expertise in running model simulations.

Competing interests. no competing interests are present

Acknowledgements. This research was supported by the Deep South National Science Challenge (Grant Nos. C01X141E2 and C01X1901) and the UK Met Office for the use of the MetUM. We also ~~wish to~~ acknowledge the contribution of New Zealand eScience Infrastructure (NeSI) high-performance computing facilities to the results of this research. New Zealand's national facilities are provided by NeSI and funded jointly by NeSI's collaborator institutions and through the Ministry of Business, Innovation and Employment's Research Infrastructure programme (https://www.nesi.org.nz/, last access: 06 April 2023). We acknowledge the Cape Grim Science Program for the provision

of DMS data from Cape Grim. The Cape Grim Science Program is a collaboration between the Australian Bureau of Meteorology and ~~the~~

635   CSIRO Australia. LER appreciates support by the Rutherford Discovery Fellowships from New Zealand Government funding, administered by the Royal Society Te Apārangi.

References

Allison, L., Johnson, H., Marshall, D., and Munday, D.: Where do winds drive the Antarctic Circumpolar Current?, Geophysical Research Letters, 37, publisher: Wiley Online Library, 2010.

Anderson, T., Spall, S., Yool, A., Cipollini, P., Challenor, P., and Fasham, M.: Global fields of sea surface dimethylsulfide predicted from chlorophyll, nutrients and light, Journal of Marine Systems, 30, 1–20, 2001.

Asher, E. C., Dacey, J. W. H., Stukel, M., Long, M. C., and Tortell, P. D.: Processes driving seasonal variability in DMS, DMSP, and DMSO concentrations and turnover in coastal Antarctic waters, Limnology and Oceanography, 62, 104–124, https://doi.org/10.1002/lno.10379, _eprint: https://onlinelibrary.wiley.com/doi/pdf/10.1002/lno.10379, 2017.

Bates, T. S., Cline, J. D., Gammon, R. H., and Kelly-Hansen, S. R.: Regional and seasonal variations in the flux of oceanic dimethylsulfide to the atmosphere, Journal of Geophysical Research: Oceans, 92, 2930–2938, publisher: Wiley Online Library, 1987.

Behera, N., Swain, D., and Sil, S.: Effect of Antarctic sea ice on chlorophyll concentration in the Southern Ocean, Deep Sea Research Part II: Topical Studies in Oceanography, 178, 104 853, publisher: Elsevier, 2020.

Behrens, E. and Bostock, H.: The Response of the Subtropical Front to Changes in the Southern Hemisphere Westerly Winds—Evidence From Models and Observations, Journal of Geophysical Research: Oceans, 128, e2022JC019 139, publisher: Wiley Online Library, 2023.

Bell, T., De Bruyn, W., Miller, S., Ward, B., Christensen, K., and Saltzman, E.: Air–sea dimethylsulfide (DMS) gas transfer in the North Atlantic: evidence for limited interfacial gas exchange at high wind speed, Atmospheric Chemistry and Physics, 13, 11 073–11 087, publisher: Copernicus GmbH, 2013.

Bell, T., De Bruyn, W., Marandino, C. A., Miller, S., Law, C., Smith, M., and Saltzman, E.: Dimethylsulfide gas transfer coefficients from algal blooms in the Southern Ocean, Atmospheric Chemistry and Physics, 15, 1783–1794, publisher: Copernicus GmbH, 2015.

Bell, T. G., Porter, J. G., Wang, W.-L., Lawler, M. J., Boss, E., Behrenfeld, M. J., and Saltzman, E. S.: Predictability of Seawater DMS During the North Atlantic Aerosol and Marine Ecosystem Study (NAAMES), Frontiers in Marine Science, 7, 596 763, publisher: Frontiers Media SA, 2021.

Belviso, S., Bopp, L., Moulin, C., Orr, J. C., Anderson, T., Aumont, O., Chu, S., Elliott, S., Maltrud, M. E., and Simó, R.: Comparison of global climatological maps of sea surface dimethyl sulfide, Global Biogeochemical Cycles, 18, https://doi.org/10.1029/2003GB002193, publisher: American Geophysical Union, 2004.

Belviso, S., Masotti, I., Tagliabue, A., Bopp, L., Brockmann, P., Fichot, C., Caniaux, G., Prieur, L., Ras, J., Uitz, J., Loisel, H., Dessailly, D., Alvain, S., Kasamatsu, N., and Fukuchi, M.: DMS dynamics in the most oligotrophic subtropical zones of the global ocean, Biogeochemistry, 110, 215–241, https://doi.org/10.1007/s10533-011-9648-1, 2012.

Bennartz, R. and Rausch, J.: Global and regional estimates of warm cloud droplet number concentration based on 13 years of AQUA-MODIS observations, Atmospheric Chemistry and Physics, 17, 9815–9836, https://doi.org/10.5194/acp-17-9815-2017, publisher: Copernicus GmbH, 2017.

Berndt, T., Scholz, W., Mentler, B., Fischer, L., Hoffmann, E. H., Tilgner, A., Hyttinen, N., Prisle, N. L., Hansel, A., and Herrmann, H.: Fast peroxy radical isomerization and OH recycling in the reaction of OH radicals with dimethyl sulfide, The Journal of Physical Chemistry Letters, 10, 6478–6483, publisher: ACS Publications, 2019.

Berresheim, H.: Biogenic sulfur emissions from the Subantarctic and Antarctic Oceans, Journal of Geophysical Research: Atmospheres, 92, 13 245–13 262, publisher: Wiley Online Library, 1987.

Berresheim, H., Huey, J., Thorn, R., Eisele, F., Tanner, D., and Jefferson, A.: Measurements of dimethyl sulfide, dimethyl sulfoxide, dimethyl sulfone, and aerosol ions at Palmer Station, Antarctica, Journal of Geophysical Research: Atmospheres, 103, 1629–1637, publisher: Wiley Online Library, 1998.

Bhatti, Y. A., Revell, L. E., and McDonald, A. J.: Influences of Antarctic ozone depletion on Southern Ocean aerosols, Journal of Geophysical Research: Atmospheres, 127, e2022JD037 199, publisher: Wiley Online Library, 2022.

Blomquist, B. W., Brumer, S. E., Fairall, C. W., Huebert, B. J., Zappa, C. J., Brooks, I. M., Yang, M., Bariteau, L., Prytherch, J., Hare, J. E., and others: Wind speed and sea state dependencies of air-sea gas transfer: Results from the High Wind speed Gas exchange Study (HiWinGS), Journal of Geophysical Research: Oceans, 122, 8034–8062, publisher: Wiley Online Library, 2017.

Bock, J., Michou, M., Nabat, P., Abe, M., Mulcahy, J. P., Olivié, D. J., Schwinger, J., Suntharalingam, P., Tjiputra, J., Van Hulten, M., and others: Evaluation of ocean dimethylsulfide concentration and emission in CMIP6 models, Biogeosciences, 18, 3823–3860, publisher: Copernicus GmbH, 2021.

Boyd, P. and Law, C.: The Southern Ocean iron release experiment (SOIREE)—introduction and summary, Deep Sea Research Part II: Topical Studies in Oceanography, 48, 2425–2438, publisher: Elsevier, 2001.

Bracegirdle, T., Holmes, C., Hosking, J., Marshall, G., Osman, M., Patterson, M., and Rackow, T.: Improvements in circumpolar Southern Hemisphere extratropical atmospheric circulation in CMIP6 compared to CMIP5, Earth and Space Science, 7, e2019EA001 065, 2020a.

Bracegirdle, T. J., Krinner, G., Tonelli, M., Haumann, F. A., Naughten, K. A., Rackow, T., Roach, L. A., and Wainer, I.: Twenty first century changes in Antarctic and Southern Ocean surface climate in CMIP6, Atmospheric Science Letters, 21, e984, https://doi.org/10.1002/asl.984, 2020b.

Browning, T. J., Stone, K., Bouman, H. A., Mather, T. A., Pyle, D. M., Moore, C. M., and Martinez-Vicente, V.: Volcanic ash supply to the surface ocean—remote sensing of biological responses and their wider biogeochemical significance, Frontiers in Marine Science, 2, 14, publisher: Frontiers Media SA, 2015.

Choudhury, G. and Tesche, M.: A first global height-resolved cloud condensation nuclei data set derived from spaceborne lidar measurements, Earth System Science Data, 15, 3747–3760, https://doi.org/10.5194/essd-15-3747-2023, publisher: Copernicus GmbH, 2023.

Curson, A. R. J., Todd, J. D., Sullivan, M. J., and Johnston, A. W. B.: Catabolism of dimethylsulphoniopropionate: microorganisms, enzymes and genes, Nature Reviews Microbiology, 9, 849–859, https://doi.org/10.1038/nrmicro2653, number: 12 Publisher: Nature Publishing Group, 2011.

Deppeler, S. L. and Davidson, A. T.: Southern Ocean phytoplankton in a changing climate, Frontiers in Marine Science, 4, 40, publisher: Frontiers Media SA, 2017.

Elliott, S.: Dependence of DMS global sea-air flux distribution on transfer velocity and concentration field type, Journal of Geophysical Research: Biogeosciences, 114, publisher: Wiley Online Library, 2009.

Fairall, C., Yang, M., Bariteau, L., Edson, J., Helmig, D., McGillis, W., Pezoa, S., Hare, J., Huebert, B., and Blomquist, B.: Implementation of the Coupled Ocean-Atmosphere Response Experiment flux algorithm with CO2, dimethyl sulfide, and O3, Journal of Geophysical Research: Oceans, 116, publisher: Wiley Online Library, 2011.

Fan, J., Ghan, S., Ovchinnikov, M., Liu, X., Rasch, P. J., and Korolev, A.: Representation of Arctic mixed-phase clouds and the Wegener-Bergeron-Findeisen process in climate models: Perspectives from a cloud-resolving study, Journal of Geophysical Research: Atmospheres, 116, publisher: Wiley Online Library, 2011.

Fiddes, S. L., Protat, A., Mallet, M. D., Alexander, S. P., and Woodhouse, M. T.: Southern Ocean cloud and shortwave radiation biases in a nudged climate model simulation: does the model ever get it right?, Atmospheric Chemistry and Physics, 22, 14 603–14 630, publisher: Copernicus GmbH, 2022.

Fossum, K. N., Ovadnevaite, J., Ceburnis, D., Preißler, J., Snider, J. R., Huang, R.-J., Zuend, A., and O'Dowd, C.: Sea-spray regulates sulfate cloud droplet activation over oceans, npj Climate and Atmospheric Science, 3, 1–6, https://doi.org/10.1038/s41612-020-0116-2, number: 1 Publisher: Nature Publishing Group, 2020.

Galí, M., Levasseur, M., Devred, E., Simó, R., and Babin, M.: Sea-surface dimethylsulfide (DMS) concentration from satellite data at global and regional scales, Biogeosciences, 15, 3497–3519, publisher: Copernicus GmbH, 2018.

Galí, M., Devred, E., Babin, M., and Levasseur, M.: Decadal increase in Arctic dimethylsulfide emission, Proceedings of the National Academy of Sciences, 116, 19 311–19 317, publisher: National Acad Sciences, 2019.

Galí, M., Lizotte, M., Kieber, D. J., Randelhoff, A., Hussherr, R., Xue, L., Dinasquet, J., Babin, M., Rehm, E., and Levasseur, M.: DMS emissions from the Arctic marginal ice zone, Elem Sci Anth, 9, 00 113, publisher: University of California Press, 2021.

Gantt, B., Meskhidze, N., Facchini, M., Rinaldi, M., Ceburnis, D., and O'Dowd, C.: Wind speed dependent size-resolved parameterization for the organic mass fraction of sea spray aerosol, Atmospheric Chemistry and Physics, 11, 8777–8790, publisher: Copernicus Publications Göttingen, Germany, 2011.

Gantt, B., Johnson, M., Meskhidze, N., Sciare, J., Ovadnevaite, J., Ceburnis, D., and O'Dowd, C.: Model evaluation of marine primary organic aerosol emission schemes, Atmospheric Chemistry and Physics, 12, 8553–8566, publisher: Copernicus GmbH, 2012.

Goddijn-Murphy, L., Woolf, D. K., Callaghan, A. H., Nightingale, P. D., and Shutler, J. D.: A reconciliation of empirical and mechanistic models of the air-sea gas transfer velocity, Journal of Geophysical Research: Oceans, 121, 818–835, publisher: Wiley Online Library, 2016.

Gregg, W. W. and Casey, N. W.: Sampling biases in MODIS and SeaWiFS ocean chlorophyll data, Remote Sensing of Environment, 111, 25–35, publisher: Elsevier, 2007.

Gros, V., Bonsang, B., Sarda-Estève, R., Nikolopoulos, A., Metfies, K., Wietz, M., and Peeken, I.: Concentrations of dissolved dimethyl sulfide (DMS), methanethiol and other trace gases in context of microbial communities from the temperate Atlantic to the Arctic Ocean, Biogeosciences, 20, 851–867, https://doi.org/10.5194/bg-20-851-2023, publisher: Copernicus GmbH, 2023.

Grosvenor, D. P., Sourdeval, O., Zuidema, P., Ackerman, A., Alexandrov, M. D., Bennartz, R., Boers, R., Cairns, B., Chiu, J. C., Christensen, M., Deneke, H., Diamond, M., Feingold, G., Fridlind, A., Hünerbein, A., Knist, C., Kollias, P., Marshak, A., McCoy, D., Merk, D., Painemal, D., Rausch, J., Rosenfeld, D., Russchenberg, H., Seifert, P., Sinclair, K., Stier, P., van Diedenhoven, B., Wendisch, M., Werner, F., Wood, R., Zhang, Z., and Quaas, J.: Remote Sensing of Droplet Number Concentration in Warm Clouds: A Review of the Current State of Knowledge and Perspectives, Reviews of Geophysics, 56, 409–453, https://doi.org/10.1029/2017RG000593, _eprint: https://onlinelibrary.wiley.com/doi/pdf/10.1029/2017RG000593, 2018.

Hajima, T., Watanabe, M., Yamamoto, A., Tatebe, H., Noguchi, M. A., Abe, M., Ohgaito, R., Ito, A., Yamazaki, D., Okajima, H., and others: Development of the MIROC-ES2L Earth system model and the evaluation of biogeochemical processes and feedbacks, Geoscientific Model Development, 13, 2197–2244, publisher: Copernicus GmbH, 2020.

Hayashida, H., Carnat, G., Galí, M., Monahan, A. H., Mortenson, E., Sou, T., and Steiner, N. S.: Spatiotemporal variability in modeled bottom ice and sea surface dimethylsulfide concentrations and fluxes in the Arctic during 1979–2015, Global Biogeochemical Cycles, 34, e2019GB006 456, publisher: Wiley Online Library, 2020.

Haëntjens, N., Boss, E., and Talley, L. D.: Revisiting O cean C olor algorithms for chlorophyll a and particulate organic carbon in the S outhern O cean using biogeochemical floats, Journal of Geophysical Research: Oceans, 122, 6583–6593, publisher: Wiley Online Library, 2017.

Hersbach, H., Bell, B., Berrisford, P., Hirahara, S., Horányi, A., Muñoz-Sabater, J., Nicolas, J., Peubey, C., Radu, R., Schepers, D., and others: The ERA5 global reanalysis, Quarterly Journal of the Royal Meteorological Society, 146, 1999–2049, publisher: Wiley Online Library, 2020.

Ho, D. T., Law, C. S., Smith, M. J., Schlosser, P., Harvey, M., and Hill, P.: Measurements of air-sea gas exchange at high wind speeds in the Southern Ocean: Implications for global parameterizations, Geophysical Research Letters, 33, https://doi.org/10.1029/2006gl026817, 2006.

Horowitz, L. W., Naik, V., Paulot, F., Ginoux, P. A., Dunne, J. P., Mao, J., Schnell, J., Chen, X., He, J., John, J. G., Lin, M., Lin, P., Malyshev, S., Paynter, D., Shevliakova, E., and Zhao, M.: The GFDL Global Atmospheric Chemistry–Climate Model AM4.1: Model Description and Simulation Characteristics, Journal of Advances in Modeling Earth Systems, 12, e2019MS002 032, https://doi.org/https://doi.org/10.1029/2019MS002032, publisher: John Wiley & Sons, Ltd, 2020.

Hu, C., Feng, L., Lee, Z., Franz, B. A., Bailey, S. W., Werdell, P. J., and Proctor, C. W.: Improving satellite global chlorophyll a data products through algorithm refinement and data recovery, Journal of Geophysical Research: Oceans, 124, 1524–1543, publisher: Wiley Online Library, 2019.

Huebert, B. J., Blomquist, B. W., Yang, M. X., Archer, S. D., Nightingale, P. D., Yelland, M. J., Stephens, J., Pascal, R. W., and Moat, B. I.: Linearity of DMS transfer coefficient with both friction velocity and wind speed in the moderate wind speed range, Geophysical Research Letters, 37, https://doi.org/10.1029/2009GL041203, _eprint: https://onlinelibrary.wiley.com/doi/pdf/10.1029/2009GL041203, 2010.

Hulswar, S., Simó, R., Gali Tapias, M., Bell, T. G., Lana, A., Inamdar, S., Halloran, P. R., Manville, G., and Mahajan, A. S.: Third revision of the global surface seawater dimethyl sulfide climatology (DMS-Rev3), Earth System Science Data, 14, 2963–2987, publisher: Copernicus Publications, 2022.

Jarníková, T. and Tortell, P. D.: Towards a revised climatology of summertime dimethylsulfide concentrations and sea–air fluxes in the Southern Ocean, Environmental Chemistry, 13, 364, https://doi.org/10.1071/EN14272, 2016.

Jena, B.: The effect of phytoplankton pigment composition and packaging on the retrieval of chlorophyll-a concentration from satellite observations in the Southern Ocean, International Journal of Remote Sensing, 38, 3763–3784, publisher: Taylor & Francis, 2017.

Johnson, R., Strutton, P. G., Wright, S. W., McMinn, A., and Meiners, K. M.: Three improved satellite chlorophyll algorithms for the Southern Ocean, Journal of Geophysical Research: Oceans, 118, 3694–3703, publisher: Wiley Online Library, 2013.

Keller, M. D., Bellows, W. K., and Guillard, R. R.: Dimethyl sulfide production in marine phytoplankton, ACS Publications, 1989.

Kettle, A., Andreae, M. O., Amouroux, D., Andreae, T., Bates, T., Berresheim, H., Bingemer, H., Boniforti, R., Curran, M., DiTullio, G., and others: A global database of sea surface dimethylsulfide (DMS) measurements and a procedure to predict sea surface DMS as a function of latitude, longitude, and month, Global Biogeochemical Cycles, 13, 399–444, publisher: Wiley Online Library, 1999.

Kiene, R. P. and Bates, T. S.: Biological removal of dimethyl sulphide from sea water, Nature, 345, 702–705, 1990.

Kloster, S., Feichter, J., Maier-Reimer, E., Six, K. D., Stier, P., and Wetzel, P.: DMS cycle in the marine ocean-atmosphere system–a global model study, Biogeosciences, 3, 29–51, publisher: Copernicus GmbH, 2006.

Korhonen, H., Carslaw, K. S., Spracklen, D. V., Mann, G. W., and Woodhouse, M. T.: Influence of oceanic dimethyl sulfide emissions on cloud condensation nuclei concentrations and seasonality over the remote Southern Hemisphere oceans: A global model study, Journal of Geophysical Research, 113, https://doi.org/10.1029/2007jd009718, 2008.

Kremser, S., Harvey, M., Kuma, P., Hartery, S., Saint-Macary, A., McGregor, J., Schuddeboom, A., Von Hobe, M., Lennartz, S. T., Geddes, A., and others: Southern Ocean cloud and aerosol data: a compilation of measurements from the 2018 Southern Ocean Ross Sea Marine Ecosystems and Environment voyage, Earth System Science Data, 13, 3115–3153, publisher: Copernicus GmbH, 2021.

Kuma, P., McDonald, A. J., Morgenstern, O., Alexander, S. P., Cassano, J. J., Garrett, S., Halla, J., Hartery, S., Harvey, M. J., Parsons, S., and others: Evaluation of Southern Ocean cloud in the HadGEM3 general circulation model and MERRA-2 reanalysis using ship-based observations, Atmospheric Chemistry and Physics, 20, 6607–6630, publisher: Copernicus GmbH, 2020.

Lana, A., Bell, T., Simó, R., Vallina, S., Ballabrera-Poy, J., Kettle, A., Dachs, J., Bopp, L., Saltzman, E., Stefels, J., and others: An updated climatology of surface dimethylsulfide concentrations and emission fluxes in the global ocean, Global Biogeochemical Cycles, 25, publisher: Wiley Online Library, 2011.

Law, C. S., Smith, M. J., Harvey, M. J., Bell, T. G., Cravigan, L. T., Elliott, F. C., Lawson, S. J., Lizotte, M., Marriner, A., McGregor, J., and others: Overview and preliminary results of the Surface Ocean Aerosol Production (SOAP) campaign, Atmospheric Chemistry and Physics, 17, 13 645–13 667, publisher: Copernicus GmbH, 2017.

Lee, G., Park, J., Jang, Y., Lee, M., Kim, K.-R., Oh, J.-R., Kim, D., Yi, H.-I., and Kim, T.-Y.: Vertical variability of seawater DMS in the South Pacific Ocean and its implication for atmospheric and surface seawater DMS, Chemosphere, 78, 1063–1070, publisher: Elsevier, 2010.

Li, F., Vikhliaev, Y. V., Newman, P. A., Pawson, S., Perlwitz, J., Waugh, D. W., and Douglass, A. R.: Impacts of interactive stratospheric chemistry on Antarctic and Southern Ocean climate change in the Goddard Earth Observing System, version 5 (GEOS-5), Journal of Climate, 29, 3199–3218, 2016.

Liss, P. S. and Merlivat, L.: Air-sea gas exchange rates: Introduction and synthesis, in: The role of air-sea exchange in geochemical cycling, pp. 113–127, Springer, 1986.

Longman, J., Palmer, M. R., Gernon, T. M., Manners, H. R., and Jones, M. T.: Subaerial volcanism is a potentially major contributor to oceanic iron and manganese cycles, Communications Earth & Environment, 3, 60, publisher: Nature Publishing Group UK London, 2022.

Madec, G. and others: NEMO ocean engine, version 3.0, Note du Pôle de modélisation de l'Institut Pierre-Simon Laplace, 27, 217, 2008.

Mann, G., Carslaw, K., Ridley, D., Spracklen, D., Pringle, K., Merikanto, J., Korhonen, H., Schwarz, J., Lee, L., Manktelow, P., and others: Intercomparison of modal and sectional aerosol microphysics representations within the same 3-D global chemical transport model, Atmospheric Chemistry and Physics, 12, 4449–4476, publisher: Copernicus GmbH, 2012.

Mann, G. W., Carslaw, K. S., Spracklen, D. V., Ridley, D. A., Manktelow, P. T., Chipperfield, M. P., Pickering, S. J., and Johnson, C. E.: Description and evaluation of GLOMAP-mode: a modal global aerosol microphysics model for the UKCA composition-climate model, Geoscientific Model Development, 3, 519–551, https://doi.org/10.5194/gmd-3-519-2010, 2010.

Marandino, C., De Bruyn, W. J., Miller, S., and Saltzman, E.: Open ocean DMS air/sea fluxes over the eastern South Pacific Ocean, Atmospheric Chemistry and Physics, 9, 345–356, publisher: Copernicus GmbH, 2009.

Marrari, M., Hu, C., and Daly, K.: Validation of SeaWiFS chlorophyll a concentrations in the Southern Ocean: A revisit, Remote Sensing of Environment, 105, 367–375, publisher: Elsevier, 2006.

Matrai, P. A., Balch, W. M., Cooper, D. J., and Saltzman, E. S.: Ocean color and atmospheric dimethyl sulfide: on their mesoscale variability, Journal of Geophysical Research: Atmospheres, 98, 23 469–23 476, publisher: Wiley Online Library, 1993.

Mulcahy, J. P., Johnson, C., Jones, C. G., Povey, A. C., Scott, C. E., Sellar, A., Turnock, S. T., Woodhouse, M. T., Abraham, N. L., and Andrews, M. B.: Description and evaluation of aerosol in UKESM1 and HadGEM3-GC3. 1 CMIP6 historical simulations, Geoscientific Model Development, 13, 6383–6423, 2020.

Myhre, G., Shindell, D., and Pongratz, J.: Anthropogenic and natural radiative forcing, publisher: Cambridge University Press, 2014.

Neubauer, D., Ferrachat, S., Siegenthaler-Le Drian, C., Stoll, J., Folini, D., Tegen, I., Wieners, K., Mauritsen, T., Stemmler, I., Barthel, S., and others: HAMMOZ-Consortium MPI-ESM1. 2-HAM model output prepared for CMIP6 AerChemMIP, Earth System Grid Federation, 2019.

Nightingale, P. D., Malin, G., Law, C. S., Watson, A. J., Liss, P. S., Liddicoat, M. I., Boutin, J., and Upstill-Goddard, R. C.: In situ evaluation of air-sea gas exchange parameterizations using novel conservative and volatile tracers, Global Biogeochemical Cycles, 14, 373–387, publisher: Wiley Online Library, 2000.

O'Reilly, J. E. and Werdell, P. J.: Chlorophyll algorithms for ocean color sensors-OC4, OC5 & OC6, Remote sensing of environment, 229, 32–47, publisher: Elsevier, 2019.

Pandis, S. N., Russell, L. M., and Seinfeld, J. H.: The relationship between DMS flux and CCN concentration in remote marine regions, Journal of Geophysical Research: Atmospheres, 99, 16 945–16 957, publisher: Wiley Online Library, 1994.

Pithan, F., Athanase, M., Dahlke, S., Sánchez-Benítez, A., Shupe, M. D., Sledd, A., Streffing, J., Svensson, G., and Jung, T.: Nudging allows direct evaluation of coupled climate models with in-situ observations: A case study from the MOSAiC expedition, EGUsphere, pp. 1–23, publisher: Copernicus GmbH, 2022.

Platnick, S., Meyer, K. G., King, M. D., Wind, G., Amarasinghe, N., Marchant, B., Arnold, G. T., Zhang, Z., Hubanks, P. A., Holz, R. E., Yang, P., Ridgway, W. L., and Riedi, J.: The MODIS cloud optical and microphysical products: Collection 6 updates and examples from Terra and Aqua, IEEE transactions on geoscience and remote sensing : a publication of the IEEE Geoscience and Remote Sensing Society, 55, 502–525, https://doi.org/10.1109/TGRS.2016.2610522, 2017.

Preunkert, S., Legrand, M., Jourdain, B., Moulin, C., Belviso, S., Kasamatsu, N., Fukuchi, M., and Hirawake, T.: Interannual variability of dimethylsulfide in air and seawater and its atmospheric oxidation by-products (methanesulfonate and sulfate) at Dumont d'Urville, coastal Antarctica (1999–2003), Journal of Geophysical Research: Atmospheres, 112, https://doi.org/10.1029/2006JD007585, _eprint: https://onlinelibrary.wiley.com/doi/pdf/10.1029/2006JD007585, 2007.

Read, K., Lewis, A., Bauguitte, S., Rankin, A. M., Salmon, R., Wolff, E. W., Saiz-Lopez, A., Bloss, W., Heard, D., Lee, J., and others: DMS and MSA measurements in the Antarctic Boundary Layer: impact of BrO on MSA production, Atmospheric Chemistry and Physics, 8, 2985–2997, publisher: Copernicus GmbH, 2008.

Revell, L. E., Kremser, S., Hartery, S., Harvey, M., Mulcahy, J. P., Williams, J., Morgenstern, O., McDonald, A. J., Varma, V., and Bird, L.: The sensitivity of Southern Ocean aerosols and cloud microphysics to sea spray and sulfate aerosol production in the HadGEM3-GA7. 1 chemistry–climate model, Atmospheric Chemistry and Physics, 19, 15 447–15 466, 2019.

Revell, L. E., Wotherspoon, N., Jones, O., Bhatti, Y. A., Williams, J., Mackie, S., and Mulcahy, J.: Atmosphere-Ocean Feedback From Wind-Driven Sea Spray Aerosol Production, Geophysical Research Letters, 48, e2020GL091 900, 2021.

Saltzman, E., King, D., Holmen, K., and Leck, C.: Experimental determination of the diffusion coefficient of dimethylsulfide in water, Journal of Geophysical Research: Oceans, 98, 16 481–16 486, publisher: Wiley Online Library, 1993.

Salzmann, M., Ferrachat, S., Tully, C., Münch, S., Watson-Parris, D., Neubauer, D., Siegenthaler-Le Drian, C., Rast, S., Heinold, B., Crueger, T., and others: The Global Atmosphere-aerosol Model ICON-A-HAM2. 3–Initial Model Evaluation and Effects of Radiation Balance Tuning on Aerosol Optical Thickness, Journal of Advances in Modeling Earth Systems, 14, e2021MS002 699, publisher: Wiley Online Library, 2022.

Santoso, A., Mcphaden, M. J., and Cai, W.: The defining characteristics of ENSO extremes and the strong 2015/2016 El Niño, Reviews of Geophysics, 55, 1079–1129, publisher: Wiley Online Library, 2017.

860 Schollaert, S. E., Yoder, J. A., O'Reilly, J. E., and Westphal, D. L.: Influence of dust and sulfate aerosols on ocean color spectra and chlorophyll a concentrations derived from SeaWiFS off the US east coast, Journal of Geophysical Research: Oceans, 108, publisher: Wiley Online Library, 2003.

Schuddeboom, A. J. and McDonald, A. J.: The Southern Ocean Radiative Bias, Cloud Compensating Errors, and Equilibrium Climate Sensitivity in CMIP6 Models, Journal of Geophysical Research: Atmospheres, 126, e2021JD035 310, publisher: Wiley Online Library, 865 2021.

Seland, O., Bentsen, M., Oliviè, D. J. L., Toniazzo, T., Gjermundsen, A., Graff, L. S., Debernard, J. B., Gupta, A. K., He, Y., Kirkevåg, A., and others: NCC NorESM2-LM model output prepared for CMIP6 CMIP historical, Earth System Grid Federation, 10, 2019.

Seland, O., Bentsen, M., Olivié, D., Toniazzo, T., Gjermundsen, A., Graff, L. S., Debernard, J. B., Gupta, A. K., He, Y.-C., Kirkevåg, A., and others: Overview of the Norwegian Earth System Model (NorESM2) and key climate response of CMIP6 DECK, historical, and scenario 870 simulations, Geoscientific Model Development, 13, 6165–6200, publisher: Copernicus GmbH, 2020.

Sellar, A. A., Jones, C. G., Mulcahy, J. P., Tang, Y., Yool, A., Wiltshire, A., O'connor, F. M., Stringer, M., Hill, R., and Palmieri, J.: UKESM1: Description and evaluation of the UK Earth System Model, Journal of Advances in Modeling Earth Systems, 11, 4513–4558, 2019.

Shon, Z.-H., Davis, D., Chen, G., Grodzinsky, G., Bandy, A., Thornton, D., Sandholm, S., Bradshaw, J., Stickel, R., Chameides, W., and others: Evaluation of the DMS flux and its conversion to SO2 over the southern ocean, Atmospheric Environment, 35, 159–172, publisher: 875 Elsevier, 2001.

Smith, M. J., Walker, C. F., Bell, T. G., Harvey, M. J., Saltzman, E. S., and Law, C. S.: Gradient flux measurements of sea–air DMS transfer during the Surface Ocean Aerosol Production (SOAP) experiment, Atmospheric Chemistry and Physics, 18, 5861–5877, https://doi.org/10.5194/acp-18-5861-2018, 2018.

Séférian, R., Nabat, P., Michou, M., Saint-Martin, D., Voldoire, A., Colin, J., Decharme, B., Delire, C., Berthet, S., Chevallier, M., and others: 880 Evaluation of CNRM earth system model, CNRM-ESM2-1: Role of earth system processes in present-day and future climate, Journal of Advances in Modeling Earth Systems, 11, 4182–4227, publisher: Wiley Online Library, 2019.

Tang, W., Llort, J., Weis, J., Perron, M. M., Basart, S., Li, Z., Sathyendranath, S., Jackson, T., Sanz Rodriguez, E., Proemse, B. C., and others: Widespread phytoplankton blooms triggered by 2019–2020 Australian wildfires, Nature, 597, 370–375, publisher: Nature Publishing Group, 2021.

885 Tang, Y., Rumbold, S., Ellis, R., Kelley, D., Mulcahy, J., Sellar, A., Walton, J., and Jones, C.: MOHC UKESM1. 0-LL model output prepared for CMIP6 CMIP, publisher: World Data Center for Climate (WDCC) at DKRZ, 2019.

Tatebe, H. and Watanabe, M.: MIROC MIROC6 model output prepared for CMIP6 CMIP historical, https://doi.org/10.22033/ESGF/CMIP6.5603, 2018.

Telford, P., Braesicke, P., Morgenstern, O., and Pyle, J.: Description and assessment of a nudged version of the new dynamics Unified Model, 890 Atmospheric Chemistry and Physics, 8, 1701–1712, publisher: Copernicus GmbH, 2008.

Thompson, P. A., Bonham, P., Thomson, P., Rochester, W., Doblin, M. A., Waite, A. M., Richardson, A., and Rousseaux, C. S.: Climate variability drives plankton community composition changes: The 2010–2011 El Niño to La Niña transition around Australia, Journal of Plankton Research, 37, 966–984, publisher: Oxford University Press, 2015.

Tison, J.-L., Brabant, F., Dumont, I., and Stefels, J.: High-resolution dimethyl sulfide and dimethylsulfoniopropionate time series profiles in 895 decaying summer first-year sea ice at Ice Station Polarstern, western Weddell Sea, Antarctica, Journal of Geophysical Research: Biogeosciences, 115, publisher: Wiley Online Library, 2010.

Titchner, H. A. and Rayner, N. A.: The Met Office Hadley Centre sea ice and sea surface temperature data set, version 2: 1. Sea ice concentrations, Journal of Geophysical Research: Atmospheres, 119, 2864–2889, publisher: Wiley Online Library, 2014.

Tjiputra, J. F., Schwinger, J., Bentsen, M., Morée, A. L., Gao, S., Bethke, I., Heinze, C., Goris, N., Gupta, A., He, Y.-C., and others: Ocean biogeochemistry in the Norwegian Earth System Model version 2 (NorESM2), Geoscientific Model Development, 13, 2393–2431, publisher: Copernicus GmbH, 2020.

Townsend, D. W. and Keller, M. D.: Dimethylsulfide (DMS) and dimethylsulfoniopropionate (DMSP) in relation to phytoplankton in the Gulf of Maine, Marine Ecology Progress Series, 137, 229–241, 1996.

Uhlig, C., Damm, E., Peeken, I., Krumpen, T., Rabe, B., Korhonen, M., and Ludwichowski, K.-U.: Sea ice and water mass influence dimethylsulfide concentrations in the central Arctic Ocean, Frontiers in Earth Science, 7, 179, publisher: Frontiers Media SA, 2019.

Vergara-Temprado, J., Miltenberger, A. K., Furtado, K., Grosvenor, D. P., Shipway, B. J., Hill, A. A., Wilkinson, J. M., Field, P. R., Murray, B. J., and Carslaw, K. S.: Strong control of Southern Ocean cloud reflectivity by ice-nucleating particles, Proceedings of the National Academy of Sciences, 115, 2687–2692, publisher: National Acad Sciences, 2018.

Vlahos, P. and Monahan, E. C.: A generalized model for the air-sea transfer of dimethyl sulfide at high wind speeds, Geophysical Research Letters, 36, https://doi.org/10.1029/2009gl040695, 2009.

Wang, Y., Chen, H.-H., Tang, R., He, D., Lee, Z., Xue, H., Wells, M., Boss, E., and Chai, F.: Australian fire nourishes ocean phytoplankton bloom, Science of The Total Environment, 807, 150 775, publisher: Elsevier, 2022.

Wanninkhof, R.: Relationship between wind speed and gas exchange over the ocean, Journal of Geophysical Research: Oceans, 97, 7373–7382, https://doi.org/10.1029/92JC00188, 1992.

Wanninkhof, R.: Relationship between wind speed and gas exchange over the ocean revisited, Limnology and Oceanography: Methods, 12, 351–362, https://doi.org/10.4319/lom.2014.12.351, 2014.

Webb, A. v., Van Leeuwe, M., Den Os, D., Meredith, M., J Venables, H., and Stefels, J.: Extreme spikes in DMS flux double estimates of biogenic sulfur export from the Antarctic coastal zone to the atmosphere, Scientific reports, 9, 1–11, publisher: Nature Publishing Group, 2019.

Wohl, C., Brown, I., Kitidis, V., Jones, A. E., Sturges, W. T., Nightingale, P. D., and Yang, M.: Underway seawater and atmospheric measurements of volatile organic compounds in the Southern Ocean, Biogeosciences, 17, 2593–2619, publisher: Copernicus GmbH, 2020.

Wu, T., Lu, Y., Fang, Y., Xin, X., Li, L., Li, W., Jie, W., Zhang, J., Liu, Y., Zhang, L., Zhang, F., Zhang, Y., Wu, F., Li, J., Chu, M., Wang, Z., Shi, X., Liu, X., Wei, M., Huang, A., Zhang, Y., and Liu, X.: The Beijing Climate Center Climate System Model (BCC-CSM): the main progress from CMIP5 to CMIP6, Geoscientific Model Development, 12, 1573–1600, https://doi.org/10.5194/gmd-12-1573-2019, publisher: Copernicus GmbH, 2019.

Yang, M., Blomquist, B., Fairall, C., Archer, S., and Huebert, B.: Air-sea exchange of dimethylsulfide in the Southern Ocean: Measurements from SO GasEx compared to temperate and tropical regions, Journal of Geophysical Research: Oceans, 116, publisher: Wiley Online Library, 2011.

Yoder, J. A. and Kennelly, M. A.: Seasonal and ENSO variability in global ocean phytoplankton chlorophyll derived from 4 years of SeaWiFS measurements, Global Biogeochemical Cycles, 17, publisher: Wiley Online Library, 2003.

Yool, A., Popova, E. E., and Anderson, T. R.: MEDUSA-2.0: an intermediate complexity biogeochemical model of the marine carbon cycle for climate change and ocean acidification studies, Geoscientific Model Development, 6, 1767–1811, https://doi.org/10.5194/gmd-6-1767-2013, 2013.

Yool, A., Palmiéri, J., Jones, C., Sellar, A., de Mora, L., Kuhlbrodt, T., Popova, E., Mulcahy, J., Wiltshire, A., and Rumbold, S.: Spin-up of UK Earth System Model 1 (UKESM1) for CMIP6, Journal of Advances in Modeling Earth Systems, 12, e2019MS001 933, 2020.

Yool, A., Palmiéri, J., Jones, C. G., de Mora, L., Kuhlbrodt, T., Popova, E. E., Nurser, A., Hirschi, J., Blaker, A. T., and Coward, A. C.: Evaluating the physical and biogeochemical state of the global ocean component of UKESM1 in CMIP6 historical simulations, Geoscientific Model Development, 14, 3437–3472, 2021.

Yukimoto, S., Koshiro, T., Kawai, H., Oshima, N., Yoshida, K., Urakawa, S., Tsujino, H., Deushi, M., Tanaka, T., Hosaka, M., Yoshimura, H., Shindo, E., Mizuta, R., Ishii, M., Obata, A., and Adachi, Y.: MRI MRI-ESM2.0 model output prepared for CMIP6 CMIP historical, https://doi.org/10.22033/ESGF/CMIP6.6842, 2019.

Zavarsky, A., Goddijn-Murphy, L., Steinhoff, T., and Marandino, C. A.: Bubble-mediated gas transfer and gas transfer suppression of DMS and CO2, Journal of Geophysical Research: Atmospheres, 123, 6624–6647, publisher: Wiley Online Library, 2018.

Zeng, C., Xu, H., and Fischer, A. M.: Chlorophyll-a estimation around the Antarctica peninsula using satellite algorithms: hints from field water leaving reflectance, Sensors, 16, 2075, publisher: MDPI, 2016.

Zhang, M., Park, K.-T., Yan, J., Park, K., Wu, Y., Jang, E., Gao, W., Tan, G., Wang, J., and Chen, L.: Atmospheric dimethyl sulfide and its significant influence on the sea-to-air flux calculation over the Southern Ocean, Progress in Oceanography, 186, 102 392, publisher: Elsevier, 2020.

Zhao, X., Liu, X., Burrows, S. M., and Shi, Y.: Effects of marine organic aerosols as sources of immersion-mode ice-nucleating particles on high-latitude mixed-phase clouds, Atmospheric Chemistry and Physics, 21, 2305–2327, publisher: Copernicus GmbH, 2021.

Zhao, Y., Booge, D., Marandino, C. A., Schlundt, C., Bracher, A., Atlas, E. L., Williams, J., and Bange, H. W.: Dimethylated sulfur compounds in the Peruvian upwelling system, Biogeosciences, 19, 701–714, publisher: Copernicus GmbH, 2022.

Timeseries of each oceanic DMS dataset input into the simulations during DJF in the Southern Ocean. chl-a is shown with a black line. The MODIS-DMS error bars represent the standard deviation across the Southern Ocean.

DMS emissions for each simulation tracking the SOAP voyage across each hour, through time and space as a violin plot. The r^2 value compares the monthly DMS flux vs the respective oceanic DMS. Spearman's rank compares the rankings of hourly flux simulation with the rankings of hourly TAN1802 data. Each simulation overlays the corresponding SOAP voyage flux, whereby both emissions are calculated with the same sea-to-air flux, winds, and Schmidt number.

Same as Figure ??, but for TAN 2018

Scatter plot representing how DMS flux and atmospheric DMS mixing ratio respond to increasing oceanic DMS concentrations. (a-i) Each simulation presents 97920 data points within the DJF Southern Ocean. (j,k) The relationship between observational voyages during 2012 (SOAP using the Wanninkhof (2014) flux parameterization), 2019 (ANDREXII), and 2008 (SOExchange) is also presented. The r^2 value is shown on each plot to represent the coefficient of determination between the oceanic DMS and DMS emissions for each simulation and voyage.